



23103838

LIBRARY Michigan State University

This is to certify that the

thesis entitled

Synthesis and Physical Properties of Imogolite Intercalated Montmorillonite

presented by

Todd Allen Werpy

has been accepted towards fulfillment of the requirements for

M.S. degree in Chemistry

Major professor

Date June 30 /987

O-7639

PLACE IN RETURN BOX to remove this checkout from your record. TO AVOID FINES return on or before date due.

DATE DUE	DATE DUE	DATE DUE

MSU Is An Affirmative Action/Equal Opportunity Institution

SYNTHESIS AND PHYSICAL PROPERTIES OF IMOGOLITE INTERCALATED MONTMORILLONITE

Ву

Todd Allen Werpy

A THESIS

Submitted to

Michigan State University

in partial fulfillment of the requirements

for the degree of

MASTER OF SCIENCE

Department of Chemistry
1987

ABSTRACT

SYNTHESIS AND PHYSICAL PROPERTIES OF IMOGOLITE INTERCALATED MONTMORILLONITE

By

Todd Allen Werpy

The interest in smectite clays as catalysts and molecular sieves has been revitalized in recent years with the advent of pillared clays. Pillared clays, as opposed to exchanged clays offer larger interlayer spacings as well as higher thermal stability.

The major goal of this dissertation was to synthesize and characterize a new pillared smectite clay using imogolite as a pillar. Imogolite is a tubular aluminosilicate with an external diameter of 23Å and a length of approximately 1000Å.

The X-ray diffraction pattern indicated that this new imagolite-montmorillonite complex has a $d_{(001)}$ spacing of 41Å. This is the largest reported interlayer spacing of a pillared smectite to date. This complex also shows very reasonable thermal stability as evidenced by differential thermal analysis. Several other techniques were also employed in the physical characterization imagolite intercalated montmorillonite.

Based on the large interlayer spacings and good thermal stability of imogolite intercalated montmorillonite there appears to be several possible applications for this complex in the area of catalysis and as a molecular sieve.

To Julie and Courtney

ACKNOWLEDGEMENTS

I would like to thank Dr. T. J. Pinnavaia for his advice and patience during the undertaking of this project.

I hope that we can continue this relationship through the completion of my graduate studies.

I would also like to thank Dr. D. Nocera for his guidance in editing this thesis, as well as Dr. Dye for the useful suggestions he made during my oral.

Finally, I would like to thank the past and present members of my research group for their assistance and knowledge.

TABLE OF CONTENTS

CHAPT	ER	PAG	ΞE
LIST	OF TABLES	,	vi
LIST	OF FIGURES	. v	ii
CHAPT	ER I-INTRODUCTION		. 1
	Pillared Clays		. 2
	Objectives of Thesis Research		. 4
	Structure of Smectite Clay Minerals		. 5
	Swelling Properties of Smectites		. 9
	Acidity	• • :	10
	Ion Exchange in the Interlayer	• • :	11
	Physical Properties of Imogolite	• • :	14
	Chemical Properties of Imogolite	• • :	16
CHAPT	ER II-EXPERIMENTAL METHODS	• • :	18
	Clay Preparation	:	18
	X-Ray Powder Diffraction (XRD) Measurements	• • •	20
	Chemical Analysis	:	20
	BET Surface Area Measurements	:	21
	Adsorption Uptake Isotherms	:	21
	Thermal Analysis	:	21
	Infrared Spectrometry	:	22
	Synthesis and Pillaring	:	22
CHAPT	ER III-RESULTS AND DISCUSSION	:	24
	Introduction	:	24
	Characterization of Imogolite	:	24

CHAPTER	PAGE
Characterization of Imogolite Intercalated Montmorillonite	26
X-Ray Diffraction	26
Surface Area Measurements	34
Elemental Analysis	34
Thermal Analysis	36
Adsorption Isotherms	42
Conclusions	50
CHAPTER IV-FUTURE STUDIES	53
Adsorption Properties of IIM	53
Acidity	53
Catalysis	54
New Imogolite-Smectite Complexes	55
LIST OF REFERENCES	56

.

LIST OF TABLES

TABLE	PAGE
1	Idealized Structural Formulas for Some
	Dioctahedral and Trioctahedral 2:1
	Phyllosilicates7
2	Surface Area Versus Outgassing Temperature35
3	Elemental Analysis of Imogolite, Dialyzed IMM,
	Centrifuged IIM, and Na ⁺ -Montmorillonite for
	Si, Al, and Mg37
4	Pore Volumes for Dialyzed IIM and Centrifuged
	IIM Based on Kinetic Diameter of Various
	Molecules51

LIST OF FIGURES

FIGURE	PAGE
1	Schematic Representation of a Pillared Clay
	(Pinnavaia, 1983) 2
2	Schematic Representation of the Structure of
	Smectite 6
3	Idealized Structure of Imogolite,
	SiO ₂ ·Al ₂ O ₃ ·3+X H ₂ O
4	Infrared Spectrum of Imogolite. Sample
	Prepared as KBr Disk
5	X-Ray Diffraction Pattern of Imogolite Air
	Dried on a Glass Slide
6	X-Ray Diffraction Pattern of IIM Synthesized
	by Various Weight Ratios of Imogolite to
	Montmorillonite, Washed by Centrifugation:
	A=3:1, B=2:1, C=1.3:1, D=1:1, E=0.67:1
7	X-Ray diffraction Pattern of IIM Washed by
	Centrifugation, Air Dried on Glass Slides,
	and Heated to: $A=125^{\circ}C$, $B=250^{\circ}C$, $C=375^{\circ}C$,
	D=600°C31
8	X-Ray diffraction Pattern of IIM Washed by
	Dialysis, Air Dried on Glass Slides, and
	Heated to: $A=125^{\circ}C$, $B=250^{\circ}C$, $C=375^{\circ}C$,
	D=600°C

FIGURE	<u>PAGE</u>
9	DSC of Dialyzed IIM(A), Centrifuged IIM(B),
	Dialyzed Imogolite(C), and
	Na ⁺ -Montmorillonite(D). All Samples Were Air
	Dried39
10	DTA of Dialyzed IIM(A), Centrifuged IIM(B),
	Dialyzed Imogolite(C), and
	Na ⁺ -Montmorillonite(D). All Samples Were Air
	Dried41
11	TGA of Dialyzed IIM(A), Centrifuged IIM(B),
	Dialyzed Imogolite(C), and
	Na ⁺ -Montmorillonite(D). All Samples Were Air
	Dried44
12	Adsorption Isotherm of Water on Dialyzed
	IIM(O) and Centrifuged IIM()45
13	Adsorption Isotherm of Nitrogen on Dialyzed
	IIM(0) and Centrifuged IIM()46
14	Adsorption Isotherm of n-Butane on Dialyzed
	<pre>IIM(0) and Centrifuged IIM()47</pre>
15	Adsorption Isotherm of Benzene on Dialyzed
	IIM(O) and Centrifuged IIM()48
16	Adsorption Isotherm of Perfluorotribylamine on
	Dialyzed IIM(O) and Centrifuged IIM()49

CHAPTER 1

INTRODUCTION

1.1 Pillared Clays

Pillared clays are smectite minerals in which alkali metal ions in the host mineral have been replaced by thermally stable, robust cations that act as molecular props. These molecular props allow the layers to be separated in the absence of the swelling solvent[1]. Various types of cations such as alkylammonium ions[2], bicyclic amines[3], and polynuclear hydroxy metal cations[4] have been used as pillaring agents. Figure 1 is a schematic representation of a pillared clay and shows the various pillaring agents used[1].

Barrer and Mcleod[5] introduced the concept of pillared clays more than 25 years ago when they showed that permanent porosity could be introduced into montmorillonite by replacing the interlayer alkali metal with tetraalkylammonium ions. They were able to further demonstrate that pillared clays offered selective adsorption properties and could be thought of as two dimensional zeolites. Unfortunately, these materials were overshadowed by the advances being made in the synthesis and catalytic properties of zeolites. Pillared clays are now generating a renewed interest in the area of catalysis due to the development of pillars which allow the pore sizes to be larger than that of

Molecular props

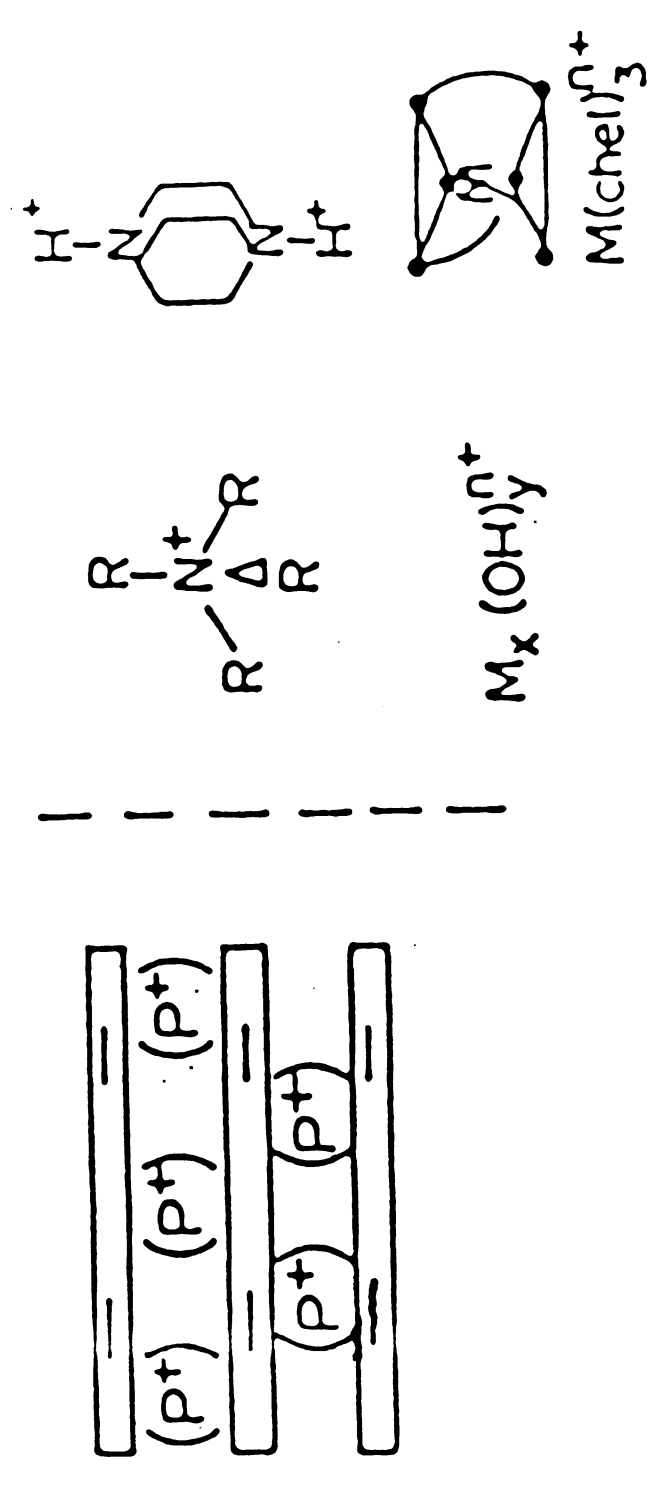


Figure 1 Schematic Representation of a Pillared Clay. (Pinnavaia, 1983)

faujasitic zeolite. In addition, the pore sizes can be made adjustable by varying the size of the pillar or the spacing between the pillars. The ability of pillared clays to have adjustable pore sizes makes them especially inviting for the catalysis of larger molecules such as those found in residual crude oil[1].

Thermal stability of pillared clays is also a very important issue. The pillaring agents illustrated in Figure 1 have very different thermal stabilities. Alkylammonium and bicyclic amine cations tend to decompose at temperatures below 250°C and metal chelates below 450°C[6]. Stability to temperatures above 500°C has been obtained by Brindley and co-workers[7,8]. They also reported hydroxy aluminum and hydroxy zirconium cations formed by base hydrolysis yielded thermally stable clays with surface areas of between 200 and $500m^2/g$.

The hydroxy zirconium pillar is an Zr_4 oligomer of the type $Zr_4(OH)^{X+}_{16-x}[8]$. The hydroxy aluminum pillar was first suggested to be an Al_6 oligomer[7], however the structure of the pillaring cation is most likely to be the Al_{13} oligomer related to the known cation $Al_{13}O_4(OH)_{24}^{7+}[9]$. This has also been reconfirmed by ^{27}Al NMR and potentiometric titration data[1].

The formation of metal oxide clusters upon dehydroxylation of hydroxy cations is what generates this remarkable stability for the Zr and Al pillared clays. In the case of ${\rm Al}_{13}$ -montmorillonite the formation of the metal oxide may be shown as

$Al_{13}O_4(OH)_{28+n}^{(3-n)+}$	-н ₂ о	$6.5 \text{ Al}_2\text{O}_3 + (3-n) \text{ H}^+$

where the aluminum is in small clusters. The exact location of the protons in the intercalate is still not known[1].

There are synthetic limitations to the preparations of oxometal species in pillared clays. These limitations are dependent upon the hydrolysis chemistry of the desired metal. The properties of the resulting clay intercalates are related to the hydrolysis chemistry and synthesis of the oxometal species[10].

1.2 Objectives of Dissertation Research

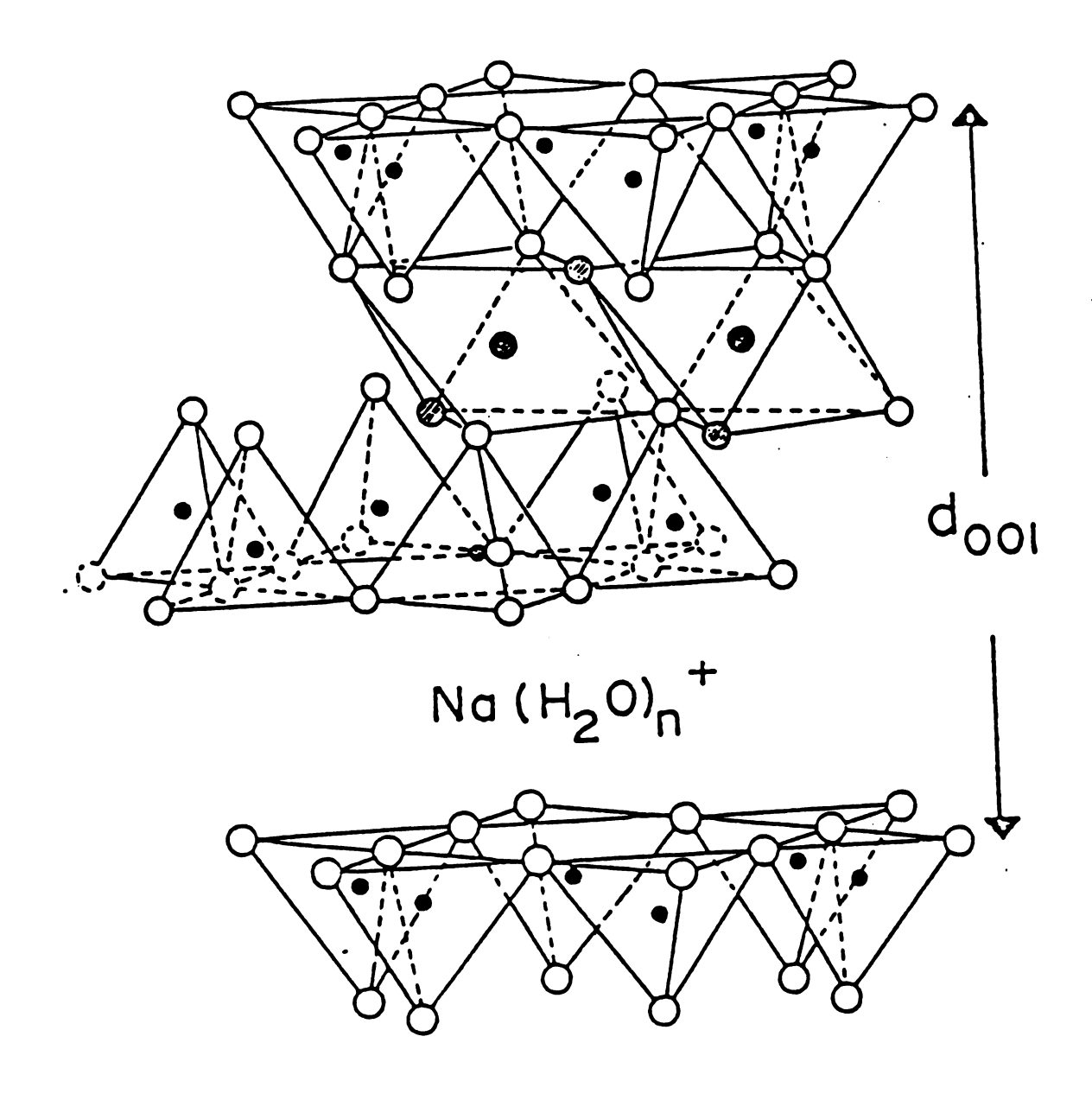
A variety of cations have been shown to permanently expand smectite-type layered silicates. Each new pillaring agent brings with it new physical and chemical properties. The purpose of this research is to evaluate an entirely new approach to the pillaring of smectite clays. This new approach is based on the direct intercalation of a neutral, molecular sized oxide in the galleries of a smectite clay. The oxide selected for study is a tubular silicate mineral known as imogolite. The second objective is to examine the adsorption properties of the new tubular silicate-layered silicate complex as a potential molecular sieve.

1.3 Structure of Smectite Clav Minerals

The term "clay" refers to a finely divided material with a particle size of less than two microns. The term "clay mineral" refers to silicate clays with definite stoichiometry and crystalline structure [11]. Figure 2 illustrates schematically the idealized structure of a smectite clay mineral layer. The oxygen atoms define upper and lower sheets of tetrahedral sites and a central sheet of octahedral sites. The relationship between the two tetrahedral sheets and one octahedral sheet within a layer allows the smectite clays to be classified as 2:1 phyllosilicates.

Two tetrahedral sheets condensed to an octahedral sheet compose a clay layer. The distance between the top of one layer and the top of an adjacent layer, encompassing the thickness of the clay layer and the height of the interlayer gallery is defined as the basal spacing. Basal spacings are defined by the d(001) reflection and can be measured by X-ray diffraction.

The different members of the smectite group of clays are distinguished by the type and location of the cations in the oxygen framework. A unit cell consists of 20 oxygen atoms and 4 hydroxyl groups, which hold eight tetrahedral sites and six octahedral sites. When two-thirds of the octahedral sites are occupied by cations, the clay is classified as a dioctahedral 2:1 phyllosilicate. If all of the octahedral sites are occupied by cations, the clay is labelled a trioctahedral 2:1 phyllosilicate. Table 1 lists



- O Oxygen
- ⊕ Hydroxyls
- . 🖪 Aluminum, Magnesium, Iron
- Silicon, Occassionaly Aluminum

Figure 2

Schematic Representation of the Structure of Smectite.

Table 1. Ideallzed Structural 2:1 Phyllosilicates.	tructural Formulas for Some Dioctahedral and Trioctahedral ilicates.	and Trioctahedral
Mineral Group	Dioctahedral	Trioctahedral
Pyrophyllite – Talc	Pyrophyllite [Al _{4.0}](Si _{8.0})0 ₂₀ (OH) ₄	Talc [Mg _{6.0}](Sig.0)20 (OH)4
Smectites.	Montmorillonite M ⁿ⁺ ·yH ₂ 0[Al4.0-x] (Si _{8.0})0 ₂₀ (0H)4	Hectorite M ⁿ⁺ .yH ₂ 0[Mg _{6.0-x} Li _x] (Si _{8.0})0 ₂₀ (OH,F) ₄
	Beidellite Mx/n·yH20[A14.0] (Si8.0-xA1x)020(0H)4	Saponite M ⁿ⁺ .yH ₂ 0[Mg _{6.0}] (Si _{8.0-x} Al _x)0 ₂₀ (0H) ₄
	Nontronite M _{x/n} ·yH ₂ 0[Fe _{4.0}] (Si _{8.0-x} Al _x)0 ₂₀ (0H) ₄	
Micas	Muscovite K ₂ [Al _{4.0}](Si _{6.0} Al ₂₀)0 _{2.0} (OH) ₄	Phylogopite K ₂ [Mg _{6.0}](Si _{6.0} Al _{2.0}) 0 ₂₀ (OH) ₄

.

idealized structural formulas for various dioctahedral and trioctahedral smectites. Included for comparison are the structural formulas for two micas (moscovite and phlogopite), pyrophyllite and talc[12].

The structure of a smectite has a framework negative charge of 44. To balance this negative charge, cations occupy the octahedral and tetrahedral sites. Obviously, differently charged cations could be used to balance this negative charge. In the case of talc all of the tetrahedral sites are occupied by Si(IV), while all octahedral sites are occupied by Mg(II). This type of occupancy leads to a neutral trioctahedral layer. The dioctahedral clay pyrophyllite obtains its electrical neutrality by the presence of Si(IV) in all eight tetrahedral holes and Al(III) in two thirds of the octahedral holes. The micas, muscovite and phlogopite have vastly different charges due to the substitution of Si(IV) by Al(III) in tetrahedral positions. This substitution results in a net negative charge of 2e per Si_8O_{20} unit which is balanced by potassium ions in the interlayer. These interlayer potassium ions coordinate to the hexagonal arrays of oxygen atoms at the layer surface.

The charge on the layers of smectites falls between talc and muscovite. The positive charge ranges from $0.4e^-$ to $1.2e^-$ per $\mathrm{Si_8O_{20}}$ unit. To balance the layer charge, layers of hydrated cation are intercalated between the silicate layers. Generally, these intercalated cations are alkaline earth ions such as Ca(II) or alkali earth metals like Na(I)[2].

1.4 Swelling Properties of Smectites

The hydration sphere associated with the interlayer cation depends in part on the hydration energy of that specific cation. The hydration energy allows the water to be ordered in the interlamellar region, usually in the layers. The extent of hydration in the clay can be measured by X-ray diffraction.

The basal spacing of dehydrated Na⁺-montmorillonite is 9.5A. As the water content increases, the spacings of 12.4, 15.4, and 18.6A are observed, corresponding to the presence of one, two, or three layers of water associated with the Na(I) ion, respectively. Further swelling can occur when Na⁺ montmorillonite is suspended in water. In fact, the aluminosilicate layers are completely dispersed, the interlayer spacing being essentially infinite.

Increasing the concentration of clay suspensions can cause gelation. This gelation phenomenon results from extensive edge-to-face and edge-to-edge layer interactions generating a "house of cards" structure [12]. This swelling phenomenon allows for the indentification of certain classes of clays. Swelling is also important to the design of clay intercalates as heterogeneous catalysts.

1.5 Acidity

Hydrated cations in smectite galleries contribute an acidic nature to the clays. The water molecules in the primary hydration sphere are polarized and partly dissociated.

$$Na^{+}(H_2O)_X$$
 \longrightarrow $Na(OH)_{x-1} + H^{+}$

The Bronsted acidity of hydrated cations in the clay galleries has been shown to be greater than that of the same cations in aqueous solution[13]. The acidity can be correlated with the cation polarizing power which increases with increasing charge-to-radius ratio. In addition, the acidity increases as the amount of interlamellar water decreases.

1.6 <u>Ion Exchange in the Interlaver</u>

Interlayer cations can be replaced through ion exchange reactions with other cations, such as organic ions[11], metal complexes[14], silicates[15], or polyoxo-inorganic cations[1]. Several of these are robust cations that act as pillars and prop the clay layers apart even without a solvent. Ion exchange reactions in the clay minerals have several characteristics in common[6]. Reaction rates generally are controlled by diffusion of the ions into the interlayer. This process occurs as the exchanging ions move against a concentration gradient. The second common characteristic is that the exchange is stoichiometric with respect to conservation of charge. Finally, ion exchange reactions are ion selective. Among homovalent cations, the smaller the effective radius, the more preferred is the binding.

The ability of clays to undergo cation exchange allows for the development of several unique intercalated compounds.

1.7 Structure of Imogolite

The name and structure of imogolite was first introduced by Yoshinga and Aomine in 1962. They had limited data available however, and were essentially able to only propose a chemical formula for imogolite with little information about its structure. The chemical formula that derived using elemental analysis 1.5SiO₂·Al₂O₃·2.5H₂O. In 1966 Wada was able to elaborate on the structure of imogolite by obtaining a relatively pure sample of imogolite. The infrared spectrum suggested a unique structure, and chemical analysis verified the presence of an oxide consisting of only SiO_2 , Al_2O_3 , and H_2O . Deuterium exchange showed the presence of surface hydroxyl groups on the fibers. In 1967 Wada proposed that imogolite was simply an end member of allophane and actually had a chemical composition ranging from SiO2·Al2O3·2H2O to allophane 2SiO₂·Al₂O₃·3H₂O. In 1969 Russel et al. used infrared and electron diffraction to further elucidate the structure of imogolite. The use of electron diffraction unambiguously showed that imogolite consisted of fibers with repeat units 8.4A parallel to the fiber axis and 23A perpendicular to it. These parameters could not be satisfied by the structure proposed by Wada in 1967. The use of infrared showed an adsorption band near 930cm⁻¹ which could be interpreted in terms of the presence of Si₂O₇ units.

Based on this evidence Russel et al.[17] proposed a layered chain structure for imogolite. However, in 1972 Cradwick, Farmer, and Russel proposed that imogolite was a hydrated aluminosilicate of tubular structure. The basis for their structure evolved from a combination of various pieces of evidence. They essentially used all of the previous data reported along with a new chemical technique which allowed them to differentiate between silicate anions with low degrees of polymerization. The technique is based on the conversion of the anion to a trimethyl silyl ether and then using gas chromatography for indentification. The application of this technique to imogolite gave products of which 95% was the orthosilicate ether and 5% was the pyrosilicate ether. Since imogolite gave such a high yield of orthosilicate ether it suggested that there is indeed an orthosilicate group in imogolite. With this additional piece of information and the other available data Cradwick, Farmer, and Russel[18] proposed the structure shown in Figure 3.

The resulting idealized chemical formula for imogolite was SiO₂·Al₂O₃·2H₂O this formula was in very good agreement with the experimental formula of 1.1SiO₂·Al₂O₃·2.5H₂O. This structure depicts how an orthosilicate anion might be associated with a gibbsite sheet. The orthosilicate anion displaces hydrogen from the three hydroxyl groups surrounding a vacant octahedral site. The fourth Si-O bond would then point directly away from the sheet and react with a proton to form SiOH. When this happens there would be a shortening of about 0.2Å in the O-O edges which define the basal plane of

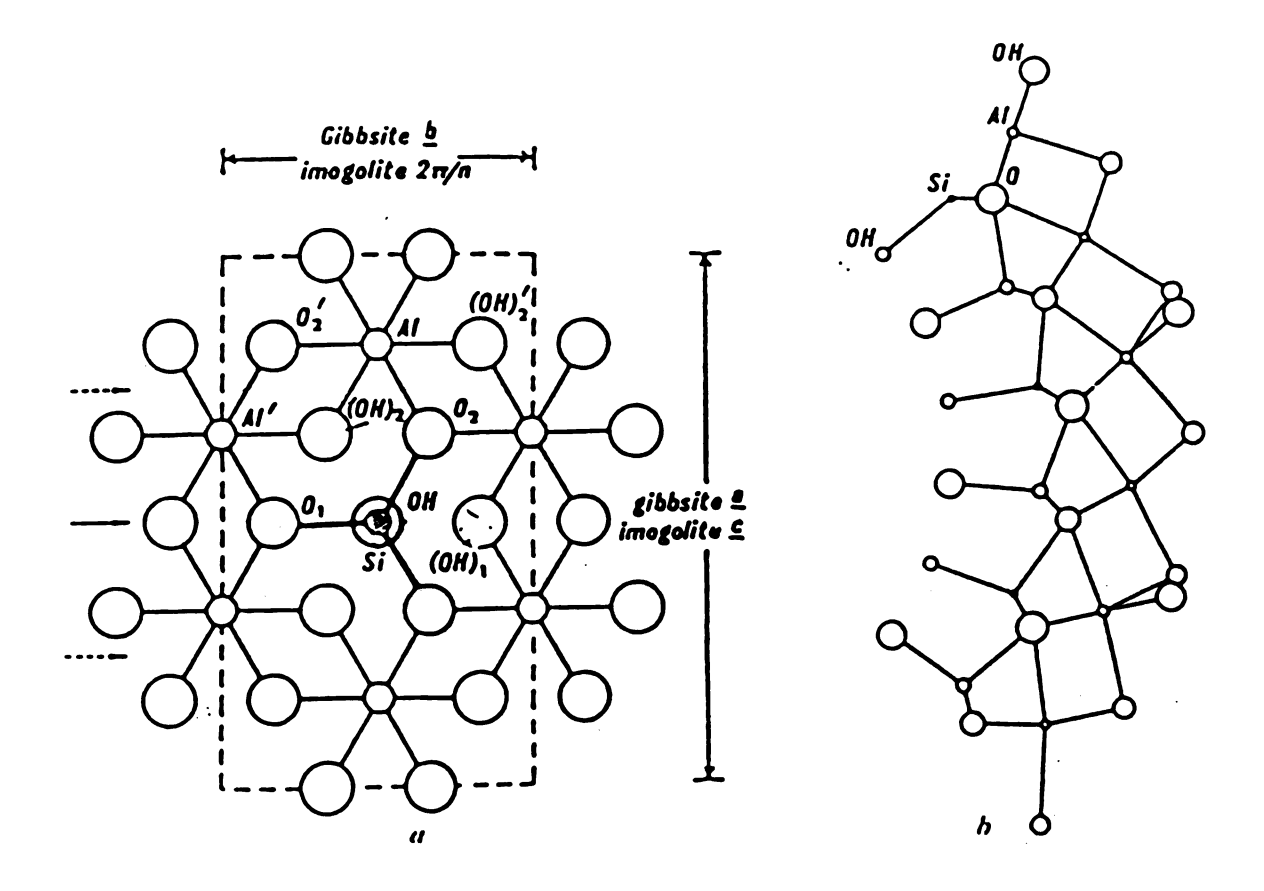


Figure 3

Idealized Structure of Imogolite, SiO₂·Al₂O₃·3+X H₂O

the tetrahedral Si site from about 3.2Å in gibbsite to less than 3Å in imagolite. This of edge lengths agrees with the shortening of the repeat unit from 8.6Å in gibbsite to 8.4Å in imogolite, as well as for the curling of the gibbsite sheet in imagolite to form a tube. These tubes would contain eleven repeat units in natural imogolite and twelve repeat units in synthetic imagolite with an outside diameter of 21 and 23A respectively[18]. This is now the accepted structure for imagolite and has since been confirmed by the use of magic angle spinning NMR[19]. The first successful synthesis of imogolite in the laboratory was performed by Farmer in 1981. Farmer synthesized imogolite by the digestion of hydroxy aluminum complexes formed at a pH of 3.2 to 5.5 in aqueous solutions with aluminum concentrations of less than 5.0 mmole per liter and silicon concentrations of less than 3.0 mmole per liter. To compare the structure of synthetic imogolite to natural imogolite Farmer used electron microscopy, electron diffraction, and infrared spectroscopy. The only difference that appeared was that synthetic imogolite was 10 to 15 percent larger than natural imogolite as expected for 12 repeat units along the circumference of the tube[20].

1.8 Physical Properties of Imogolite

The X-ray diffraction pattern of imogolite consists of several broad reflections. These reflections occur at 12-20, 7.8-8.0, and 5.5-5.6Å[21]. The X-ray diffraction pattern along with the changes that occur upon heating serve as a

good criterion for distinguishing imogolite from other clay minerals, since it has very few similarities with these minerals.

Thermal analysis is also a usful tool for characterizing imogolite. Imogolite gives a large endothermic peak between 50-300°C on the DTA curve due to a loss of large amounts of adsorbed water. Imogolite also gives an endothermic peak at 390-420°C due to dehydroxylation. The appearance of an endothermic peak at 900-1100°C is caused by imogolite changing to mullite or gamma alumina. On the TGA curve there is a continuous weight loss from 25°C to 300°C. This weight loss accounts for about 30% of the total mass of imogolite. At 300°C there is a more abrupt weight loss of about 10% due to dehydroxylation[22].

Infrared spectroscopy shows major broad adsorption in three regions, $2800-3800\,\mathrm{cm}^{-1}$, $1400-1800\,\mathrm{cm}^{-1}$, and $650-1200\,\mathrm{cm}^{-1}$. The stretching frequency in the region $2800-3800\,\mathrm{cm}^{-1}$ is attributed to OH stretching of adsorbed $\mathrm{H}_2\mathrm{O}$ or surface OH groups. An adsorption band due to the HOH deformation vibration occurs around $1630-1640\,\mathrm{cm}^{-1}$. Imagolite also shows an adsorption band at $930\,\mathrm{cm}^{-1}$ due to the Si-O stretch from the SiO₃OH group[17].

Electron diffraction of imogolite gave a series of ring reflections at 1.4, 2.1, 2.3(broad), 3.3(broad), 3.7 4.1, 5.7(broad), 11.8(broad), and 21-23Å[10,15]. The 1.4 and 2.1Å reflections were interpreted as higher order reflections arising from a repeat unit of 8.4Å along the tube axis. The 5.7, 7.8, and 11.8Å reflections were interpreted as higher

order reflections due to 21-23Å interaxial separations of the tube unit[18].

The BET surface area of imogolite was reported to be $140-170 \text{ m}^2/\text{g}$ by N₂ adsorption. This was determined by using a freeze dried sample of imogolite[17].

1.9 Chemical Properties of Imogolite

Cation exchange capacity values for natural imogolite have been hard to establish due to impurities in the soil samples. The best results were obtained by equilibrating imogolite with 0.05N NaCH₃COO at a pH of 7.0. The resulting value was 30 meq/100g. The cation exchange capacity of imogolite comes from the dissociation of surface hydroxyl groups[22].

The surface acidity of imogolite was determined by using Hammet indicators adsorbed on the clay and by titrating them in benzene suspension with n-butylamine. The H(Al) form of imogolite was found to be the most acidic while the Na-exchanged form was only slightly less acidic. Imogolite, as with most clays, was found to be more acidic at low relative humidities (ie, less than 8%). In comparison to other clays imogolite was more acidic than gibbsite, similar to Na-allophane and much less acidic than Na-montmorillonite or kaolinite. With regard to the effect of the cation on acidity it was found that H>Al>Fe>Mg>Ca>Ba>Na>NH4, this is do to the polarizing effect of the cation. The polarizing effect increases with increasing positive charge and with decreasing radius of the ion. Imogolite also shows an

increase in acidity upon heating. This is most likely due to dehydration and dehydroxylation. Imogolite reaches its most acidic state at around 500°C where dehydroxylation has essentially been completed. At 900°C there is a major loss in acidity due to new mineral formation. The acid sites of imogolite are generated by the dissociation of the surface hydroxyl groups[23].

CHAPTER II

EXPERIMENTAL

2.1 Clay Preparation

Imogolite was synthesized by the hydrolysis of $Al(t-OBu)_3$ in $HClO_3$ solution and the subsequent reaction of the resulting aluminum solution with $Si(OEt)_4$ at 95^{OC} . The general procedure has been provided previously by Farmer[18].

The naturally occurring clay mineral montmorillonite contains impurities that must be removed before exchange reactions can be undertaken. The goal is to obtain a clay that is homogeneous and free of impurities. Impurities such as soluble salts and carbonates are removed from the clay in order to enhance flocculation of the clay. Calcium carbonate should also be removed from the clay since it may prevent intercalation. It may also interfere with CEC determination due to the following equilibrium:

Sodium acetate was buffered to a pH of 5.0 with acetic acid and was used to remove carbon dioxide upon digestion at 70°C according to the following:

$$CaCO_{3(s)} + 2H^{+} \longrightarrow Ca^{2+} + H_{2}O + CO_{2(g)}$$

The exact procedure for a 5 gram clay is as follows:

- (1) Add 50 ml of 1N sodium acetate buffered with HOAc to a pH of 5.0 and bring the clay into suspension.
- (2) Digest this suspension for 1 hour at 70°C with occasional stirring.
- (3) Centrifuge the solution discard the supernatant.
- (4) Repeat the preceding steps.

Free (non-lattice) iron oxides which also inhibit exchange reactions are removed by treating the clay with sodium bicarbonate solution and subsequent low temperature (80° C) treatment with sodium thiosulfate.

- (1) Add 40 ml of 0.3N Na-citrate and 5 ml of 1N NaHCO₃. The citrate chelates with ferric iron and prevents precipitation of FeS. The bicarbonate maintains neutrality and furnishes hydroxide ion when hydrolyzed.
- (2) Warm the suspension to $75-80^{\circ}$ C and slowly add 1g of $Na_2S_2O_4$. Do not exceed 80° C or FeS may precipitate out of solution. Digest for 15 minutes. This causes the reduction of ferric ions to ferrous ions which can be washed away.
- (3) The solution is then cooled and concentrated by centrifugation and the supernatant is discarded.

Hydrogen peroxide is then added to remove organic impurities in the clay. The clay is then sodium saturated by the addition of NaCl. The flocculated particles are then

collected and washed free of chloride ion and air dried.

2.2 X-Ray Powder Diffraction

A Phillips X-ray diffractometer with Cu $K_{\rm CL}$ radiation where (λ =1.5405A) was used to measure d(001) basal spacings. All samples were prepared by allowing approximately 1ml of 1% by weight clay suspensions to air dry on a glass or quartz slide. Various samples were heated under vacuum for four hours at different temperatures. Samples which were heated over 450°C were placed on quartz slides. The Bragg angle 20 peak positions were converted to d-spacings by the use of a table relating 20 values to d-spacings. The entries in the table were calculated from the Bragg equation: $n\lambda$ =2dsin0.

2.3 Chemical Analysis

Elemental analysis of the clay samples was determined by the inorganic laboratory of the Department of Toxicology, Michigan State University. J.T. Baker instra-analyzed grade Si, Al, and Mg standards were used for for the calibration of the Jarnell-Ash auto-comp ICP emission spectrophotometer. NBS plastic clay 98a served as a clay standard. The clay samples were prepared by adding 0.05g of clay sample to 0.3g of lithium borate (Aldrich Gold Label). The samples were then mixed and fused at 1000°C for 12 minutes in preignited graphite fusion crucibles. The resultant glass was transferred to 50 ml of 6% nitric acid. This solution was mixed until complete dissolution of the glass was assured. Generally 10 minutes was a sufficient amount of time. The

solution was then diluted to 100 ml with deionized water.

2.4 BET Surface Area Measurements

Surface area measurements were determined on a Quantachrome Quantasorb Jr. at liquid nitrogen temperature with nitrogen as the adsorbate and helium as the carrier gas. The three point BET method was used for surface area determinations. The samples were outgassed at temperatures of 100, 200, 300, 400, 500, and 600°C under dynamic vacuum for 24 hours prior to nitrogen adsorption.

2.5 Adsorption Uptake Isotherms

The adsorption of organic and inorganic molecules of various kinetic diameters was measured on a McBain balance using quartz glass buckets and springs. The samples were outgassed at 350°C for 24 hours under dynamic vacuum. The probe molecules used for the adsorption were water, nitrogen, n-butane, benzene, and perfluorotributylamine with kinetic diameters of 2.65, 3.64, 4.3, 5.85, and 10.2A, respectively. The probe molecules were stirred and equilibrated in a constant temperature bath at approximately 5 degrees below room temperature. This was done to insure no capillary condensation occurred and caused erroneously high readings.

2.6 Thermal Analysis

Differential thermal analysis, differential scanning calorimetry, and thermal gravimetric analysis were carried out on a DuPont 9900 thermal analyzer. Approximately 20 mg

of sample was used for each run. The sample was ground slightly prior to the experiment for convenience. The DTA and TGA runs were recorded to a maximum temperature of 1100°C, while the DSC runs were recorded to a maximum temperature of 550°C. The ramp rate was identical for all three instruments, 10 degrees per minute. Also, all samples were run under an inert atmosphere of nitrogen.

2.7 <u>Infrared Spectrometry</u>

Infrared spectra were recorded on a Perkin Elmer model 599 spectrophotometer. The samples were KBr pellets of approximately 1% by weight. All samples were gently ground for three minutes and then pressed at 10,000 psi for 10 minutes. The scan time for recording spectra over the range from 4000cm⁻¹ to 200cm⁻¹ was 12 minutes. Samples for infrared spectroscopy were prepared by dialyzing a solution of imagolite for 5 days, followed by air drying. The dried imagolite was then made into a disk using KBr to dilute the sample. The KBr disk was approximately 10% imagolite by weight.

2.8 Synthesis and Pillaring

Imogolite was synthesized by a method analogous to that described by Farmer and Fraser[25]. Al $(t-OBu)_3$ was allowed to hydrolyze in an equivalent amount of $HClO_4$ at room temperature for 6-12 hours. To the resulting aluminum solution was added a 10% stoichiometric excess of Si $(OEt)_4$. The pH of the reaction mixture was adjusted to 5.0 by the

dropwise addition of 1.0M NaOH and then the pH was immediately readjusted to 3.5 with 1.0M acetic acid. The reaction mixture was heated at 95° C for 2 days at which time it became clear, indicating imagolite formation. The solution was then tested with NH₄OH to obtain a gel which verified the presence of imagolite[20].

A series of imogolite-montmorillonite reaction products were obtained by the dropwise addition of a 1.0 weight% suspension of Na+-montmorillonite to imogolite at several ratios of smectite to imogolite. The solutions were stirred for 3-6 hours, and the products were washed either by centrifugation or by dialysis. The centrifugation procedure required a minimum of three washings to remove the excess imogolite and other impurities. Dialysis was done using SpectrophorTM membrane tubing having as molecular weight cutoff of 12,000-14,000. The dialysis was done for a minimum of 5 days with the water being changed every hour for the first 6 hours and then every 12 hours. The final pH in both cases was between 3.9-4.1.

CHAPTER III

RESULTS AND DISCUSSION

3.1 Introduction

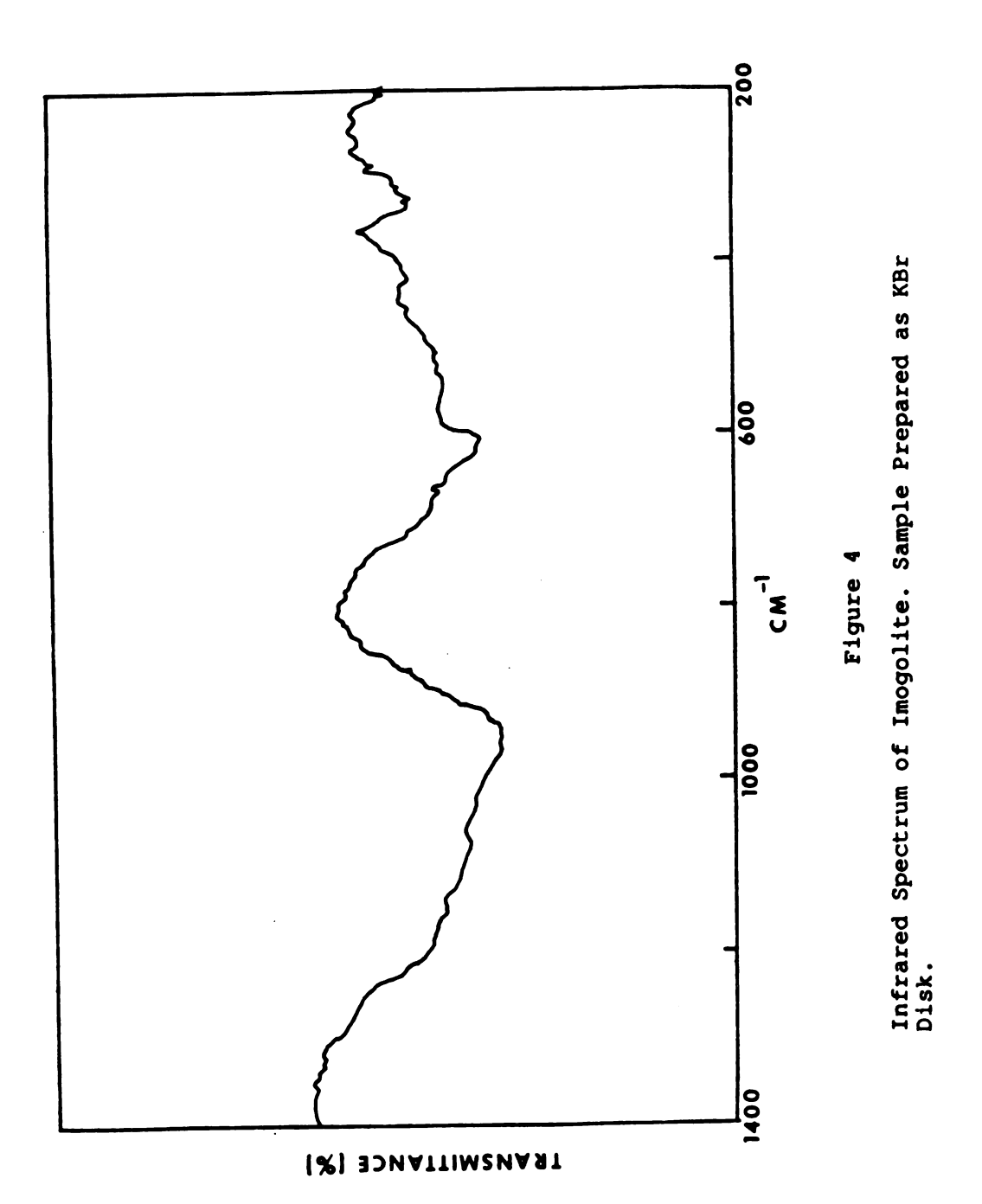
The synthesis of imogolite-intercalated montmorillonite has been recently claimed by Johnson and Pinnavaia[24].

A major objective of this work was to establish the optimum conditions for synthesis of this intercalated complex. A second objective was to determine whether or not the imagolite tubes were intercalated in the clay or somehow bound to the external surface. The final objective was to obtain some physical and chemical properties of this material and determine its potential use as a solid acid catalyst, or, possibly a shape selective catalyst. The reason for examining this material as a catalyst is because of the unique shape of imagolite and the potentially large d(001) spacings that would be obtained if the tubes are indeed intercalated.

3.2 Characterization of Imogolite

Imogolite was characterized by infrared spectroscopy, X-ray diffraction, and elemental analysis.

The infrared spectrum is shown in Figure 4. There is an adsorption band at 980cm⁻¹ indicating the presence of an orthosilicate group. There is a second adsorption band at 328cm⁻¹ which is a characteristic signature of imogolite[25]. The mode responsible for this band has not been defined.



The X-ray diffraction pattern of an imogolite film is given in Figure 5. Samples were prepared by drying imogolite suspensions on a glass slide. There are two broad peaks for imogolite, the first being at $3.9^{\circ}2\theta$ and the second at $\sim 9^{\circ}2\theta$. The peak near $9^{\circ}(8\text{\AA})$ has been attributed to the scattering of individual tubes[21]. The peak at 3.9° represents a spacing of 22.6Å and is the result of scattering by planes of close packed hexagonal arrays of tubes[21]. The apparent diameter of the tube is very close to expected value of 23\AA .

Elemental analysis was carried out on samples prepared by the procedure described in chapter II. The results indicate an Al to Si ration of 1.89. The ideal ratio would have been 2.0. However, the synthesis involves the use of excess si. Some excess Si may have been carried over due to incomplete dialysis or due to a silicon containing particle too large to be removed by dialysis.

3.3 Characterization of Imogolite Intercalated Montmorillonite

3.3.1 X-ray Diffraction

The most crystalline imogolite-montmorillonite reaction products were obtained at weight ratios of imogolite to clay in the range of 2:1 to 1.3:1. This is shown in the X-ray diffraction patterns in Figure 6. If the concentration of imogolite is to low then the X-ray diffraction pattern shows only a peak for m,ontmorillonite. At concentrations of imogolite that are greater than 2:1 then the d(001) reflection begins to disapear indicating adsorption of the tubes on the

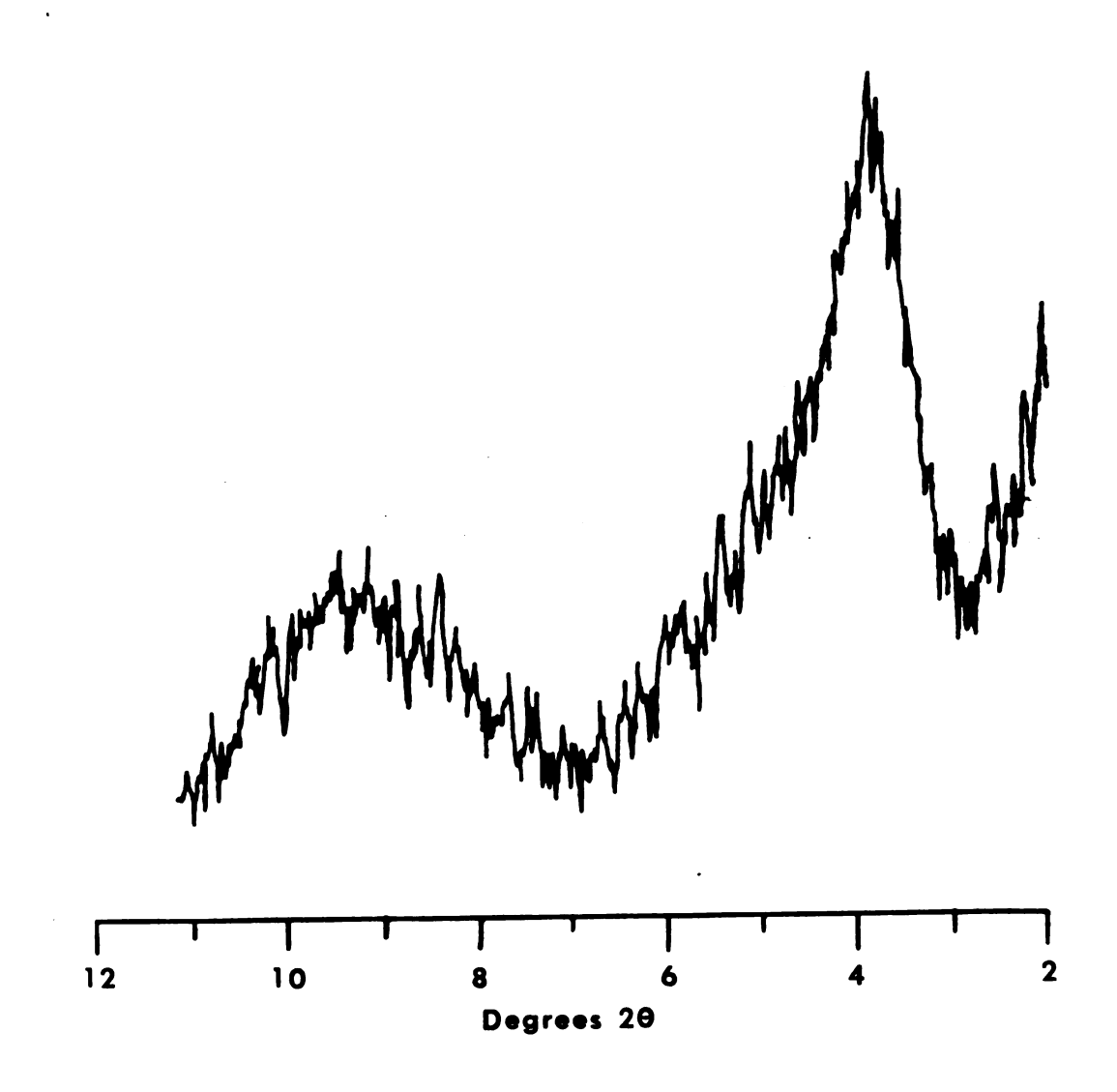


Figure 5
X-Ray Diffraction Pattern of Imogolite Air Dried on a Glass Slide.

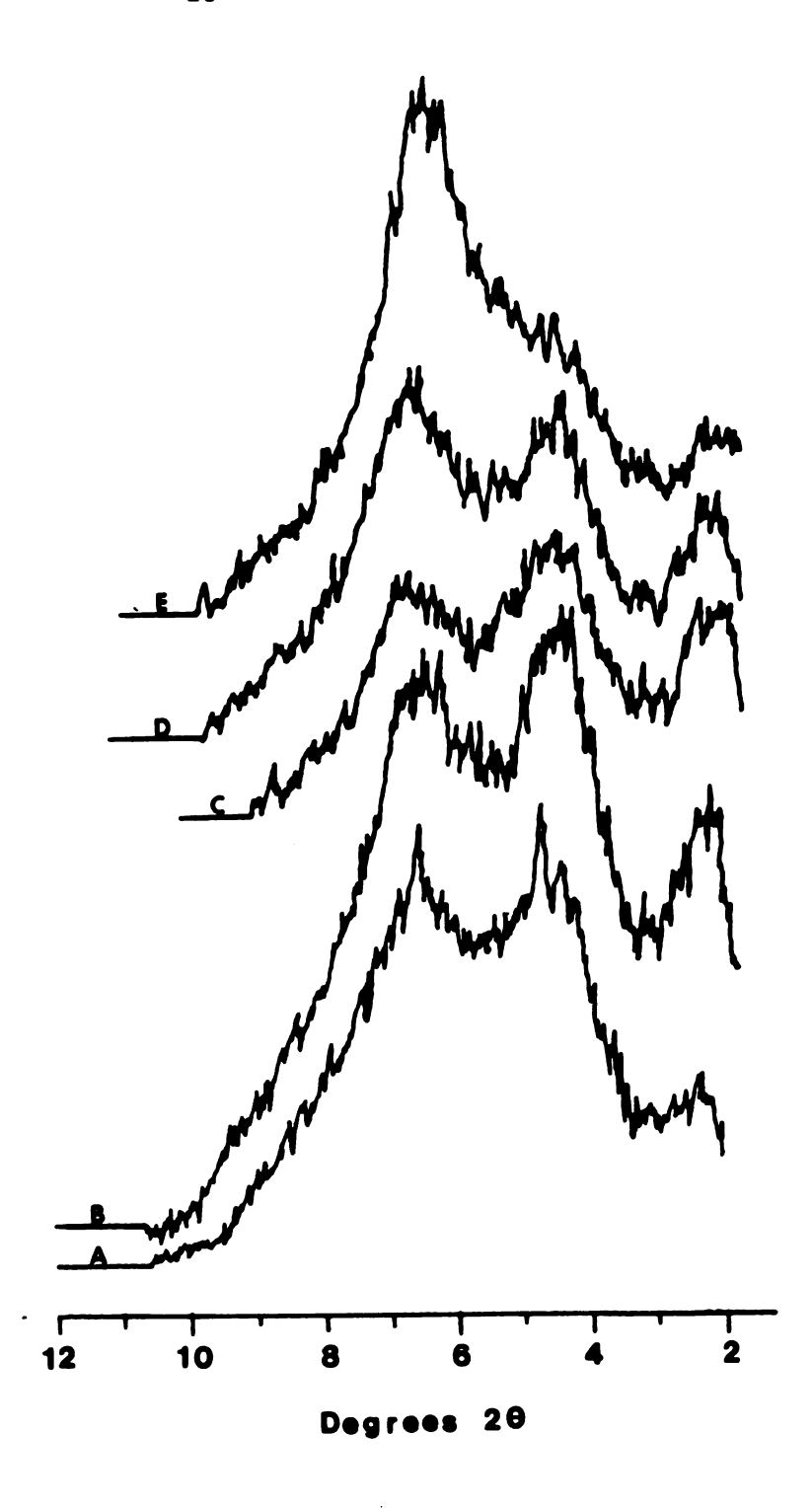


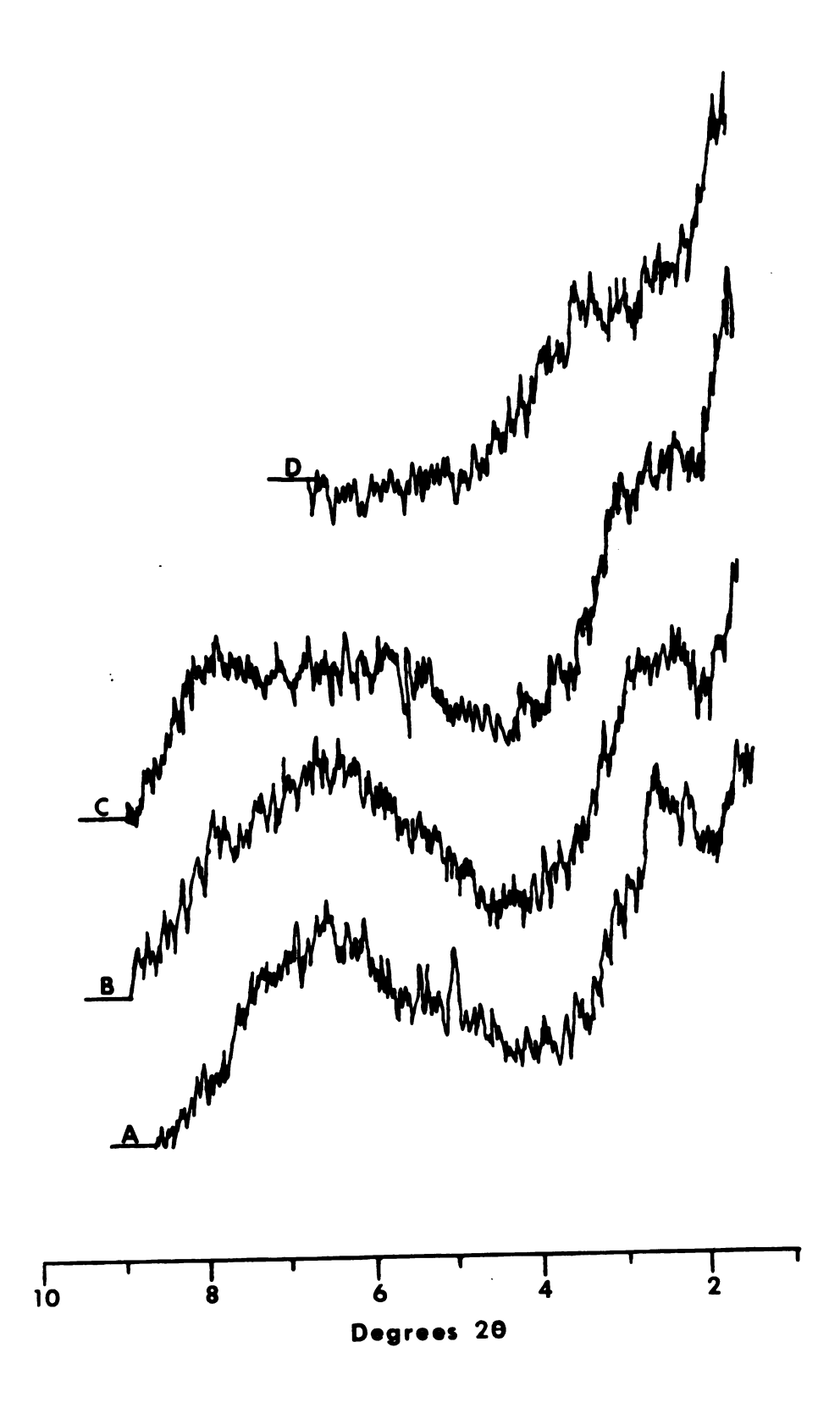
Figure 6

X-Ray Diffraction Pattern of IIM Synthesized by Various Weight Ratios of Imogolite to Montmorillonite, Washed by Centrifugation: A=3:1, B=2:1, C=1.3:1, D=1:1, E=0.67:1.

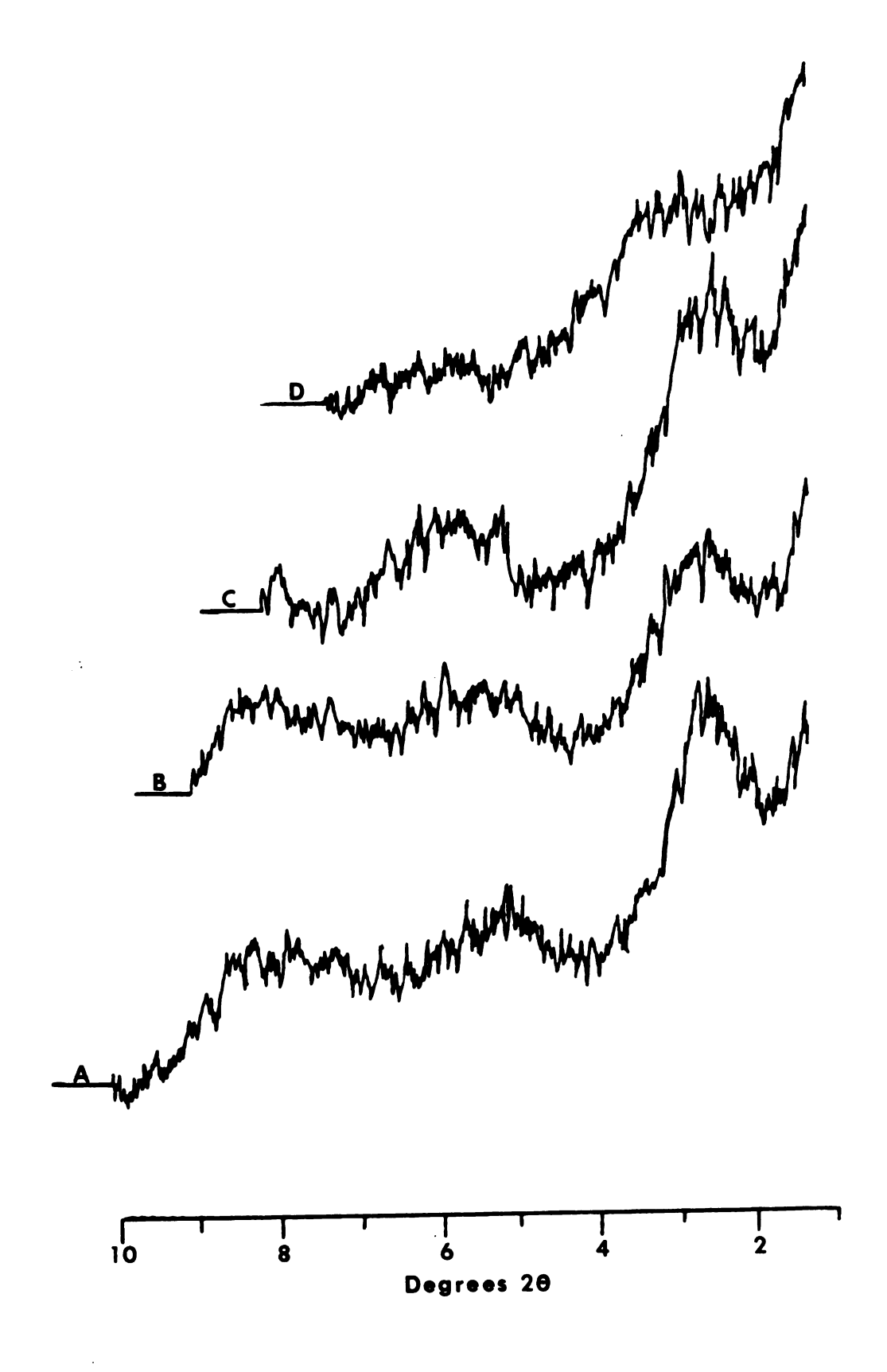
surface. Based on the crystallinity of the imogolite to montmorillonite ratio at 2:1 the synthesis appears to be at its optimum condition, therefore all remaining results are based on this synthesis. In addition X-ray diffraction was used to determine whether the imagolite was intercalated in to the galleries of the montmorillonite or simply bound to the surface. Figures 7 and 8 show the X-ray diffraction patterns of imagolite intercalated montmorillonite (IIM) for two different methods of washing. The samples in Figure 7 were washed by centrifugation while those in Figure 8 were washed by dialysis. In both figures the X-ray patterns correspond to samples heated at 125(A), 250(B), 375(C), and 600(D) or 4 hours under vacuum. The dialyzed and centrifuged samples heated at 125° C, 250° C, and 375° C show peak maxima at $2.6^{\circ}2\theta$ corresponding to a d(001) separation of 33.98Å. A separation of this magnitude would be well within the range one would expect for imagolite intercalated montmorillonite. for the tube diameter of imogolite in addition to the 12Å for the layer thickness of montmorillonite would sum to 35Å. agreement with the observed value of 34Å seems reasonable. This separation is the largest ever reported for an intercalated smectite clay.

For both the dialyzed and centrifuged samples the d(001) peak tends to broaden upon heating to 600° C, the shift in the position of d(001) to $3.6^{\circ}2\theta$ represents a d(001) spacing of 19.2Å. The decrease in layer separation may be due to the distortion or possible destruction of the imagolite tubes. The dialyzed sample seems be to more ordered than the

X-Ray Diffraction Pattern of IIM Washed by Centrifugation, Air Dried on Glass Slides, And Heated to: $A=125^{\circ}C$, $B=250^{\circ}C$, $C=375^{\circ}C$, $D=600^{\circ}C$.



X-Ray Diffraction Pattern of IIM Washed by Dialysis, Air Dried on Glass Slides, And Heated to: A=125°C, B=250°C, C=375°C, D=600°C.



centrifuged sample. For the samples heated at 125° C and 250° C there is a second order peak at $5.2^{\circ}2\theta(16.9\ \text{\AA})$ corresponding to a d value spacing of 33.9\AA . In the centrifuged samples and dialyzed samples heated above 250° C the peaks become very broad, covering $4.2^{\circ}2\theta$. The above XRD results indicate that the imagolite tubes are indeed intercalated in the montmorillonite and not just bound to the surface. In addition the complex is stable to temperature of at least 375° C.

3.3.2 Surface Area Measurements

 N_2 BET surface areas were determined for a series of dialyzed and centrifuged samples heated at temperatures of 125°C, 200°C, 300°C, 400°C, and 500°C for 16 hours under dynamic vacuum. The results of the BET surface area are shown in Table 2. The surface areas are essentially the same for both the dialyzed and centrifuged samples up to 400° C. At 500° C there is a drastic reduction in the surface area down to $80m^2/g \pm 10m^2/g$. This reduction in surface area is most likely caused by the collapsing of the imogolite tubes. This would lead to the loss of internal surface area. This lack of stability and loss of surface area may lead to problems in catalytic reactions requiring high temperatures.

3.3.3 Elemental Analysis

Elemental analysis based on Mg content showed that the imagolite-montmorillonite complex contained 61.5% imagolite and 38.5% montmorillonite. Since the complex consisted mainly

Table 2: Surface area versus outgassing temperature.

<u>Sample</u>	Temperature OC	N ₂ BET Surface Area M ² /g
Dialyzed IIM	125.0	274.5±21.0
Dialyzed IIM	200.0	250.5±20.0
Dialyzed IIM	300.0	244.0± 6.0
Dialyzed IIM	435.0	230.4±17.0
Dialyzed IIM	500.0	78.0± 5.0
Centrifuged IIM	125.0	291.9±20.7
Centrifuged IIM	200.0	309.9±15.2
Centrifuged IIM	300.0	306.0±13.0
Centrifuged IIM	435.0	274.5±14.3
Centrifuged IIM	500.0	92.4±10.3

(Surface area obtained by BET three point method at p/p_0 pressures of less than 0.10.)

of imogolite, it seems reasonable to suggest that the imogolite is not only intercalated between the clay layers, but is also bound to the surface. The values obtained from elemental analysis are given in weight% oxide in Table 3.

3.3.4 Thermal Analysis

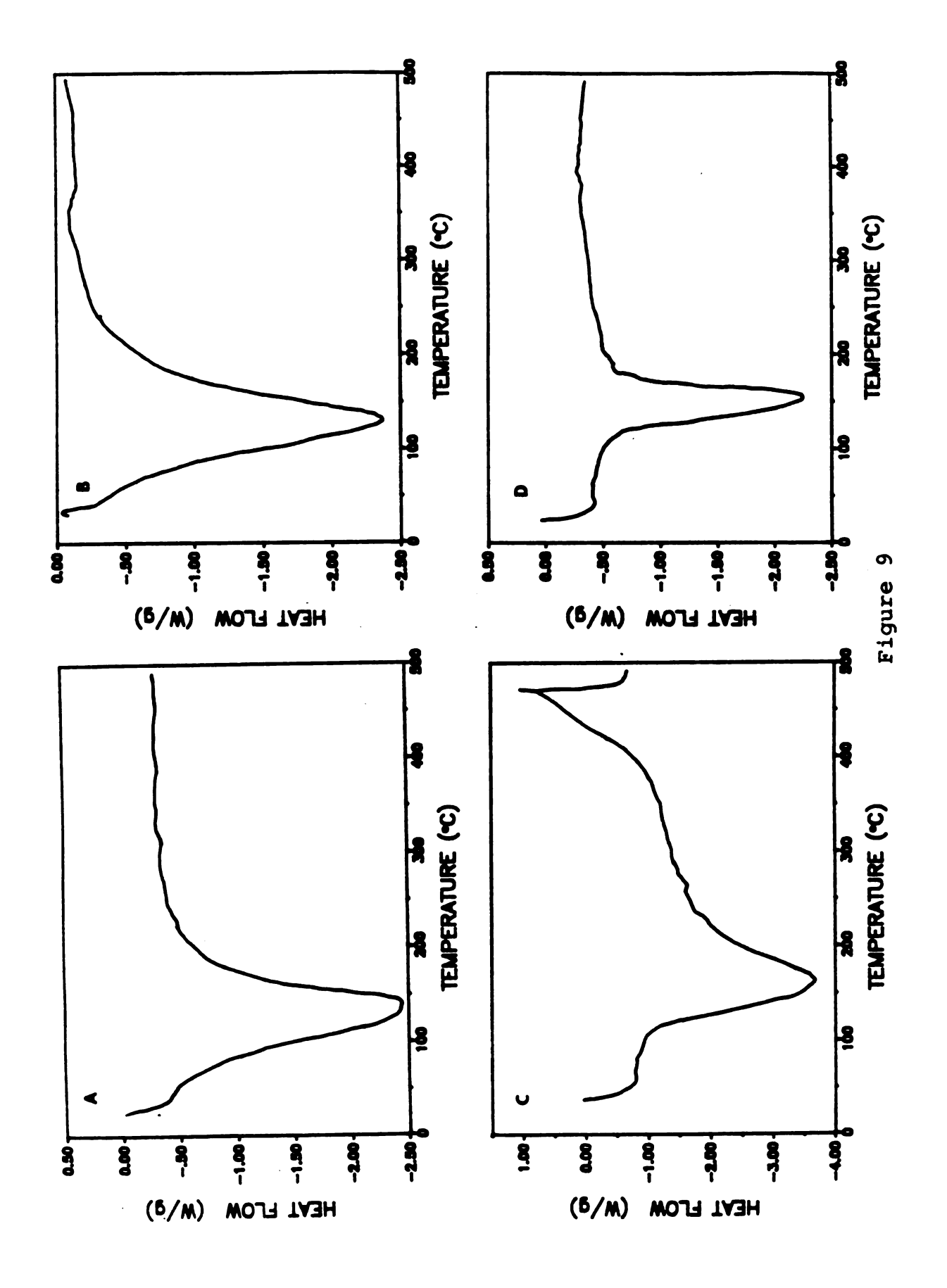
The DSC curves for dialyzed IIM(A), centrifuged IIM(B), dialyzed imogolite(C), and Na⁺-montmorillonite(D) are shown in Figure 9. Dialyzed IIM and centrifuged IIM exhibit an endothermic peak starting at 50 °C. This endotherm is due to loss of water, both from the external surface and from the interlayers. Dialyzed imogolite gives an endotherm starting at 50°C and an exotherm starting at about 350°C. endotherm is again due to a loss of water, while the exotherm caused by decomposition of imagolite. is For Na⁺-montmorillonite there is water loss starting at 60°C as shown by the presence of an endotherm. Figure 10 shows the DTA for the same samples. The DTA curves show the results identical to those obtained by DSC up to 500°C. Additional information is obtained to temperatures of 1000°C. In both dialyzed IIM and centrifuged IIM there is an endotherm at 600°C caused by surface dehydroxylation of the Na⁺-montmorillonite. The dialyzed imagolite shows an additional exotherm at 800°C due to new mineral formation. The Na⁺-montmorillonite gives rise to an exotherm at 920°C due to the formation of a new phase. The most important feature of the DSC and DTA data is that the imogolite tubes are stabilized upon intercalation into the montmorillonite layers.

Table 3: Elemental analysis of imogolite, dialyzed IIM, centrifuged IIM, and Na⁺-montmorillonite for Si, Al, and Mg.

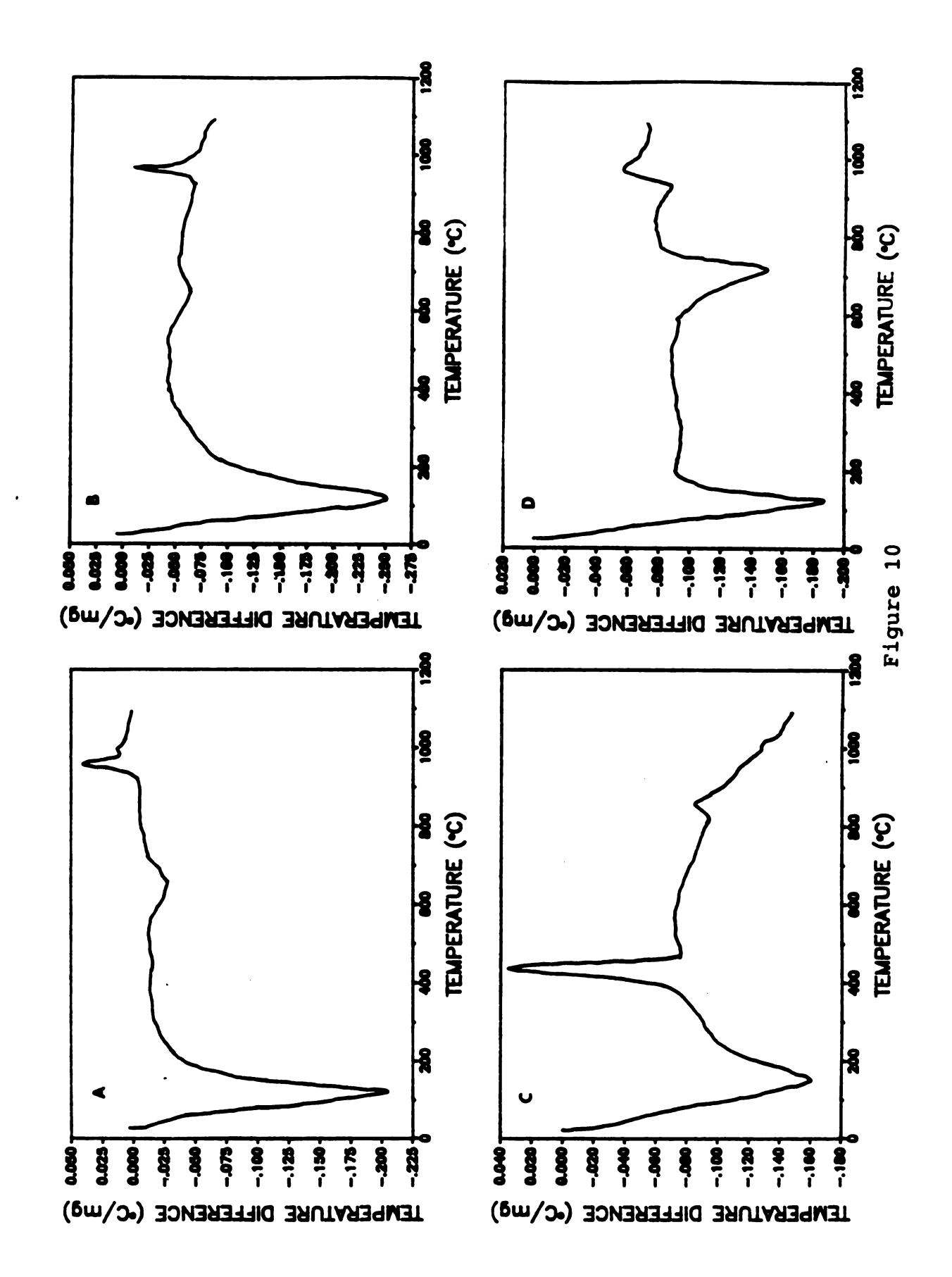
Oxide	<u>Imogolite</u>	Dial. IIM	Cent. IIM	Mont.
sio ₂	38.40	63.50	63,20	70.30
Al ₂ 0 ₃	61.60	39.78	34.92	26.04
MgO	0.0	1.72	1.76	3.66

(All values are reported in weight% of the corresponding oxide.)

DSC of Dialyzed IIM(A), Centrifuged IIM(B). Dialyzed Imogolite(C), and Na $^+$ -Montmorillonite(D). All Samples Were Air Dried.



DTA of Dialyzed IIM(A), Centrifuged IIM(B). Dialyzed Imogolite(C), and Na⁺-Montmorillonite(D). All Samples Were Air Dried.

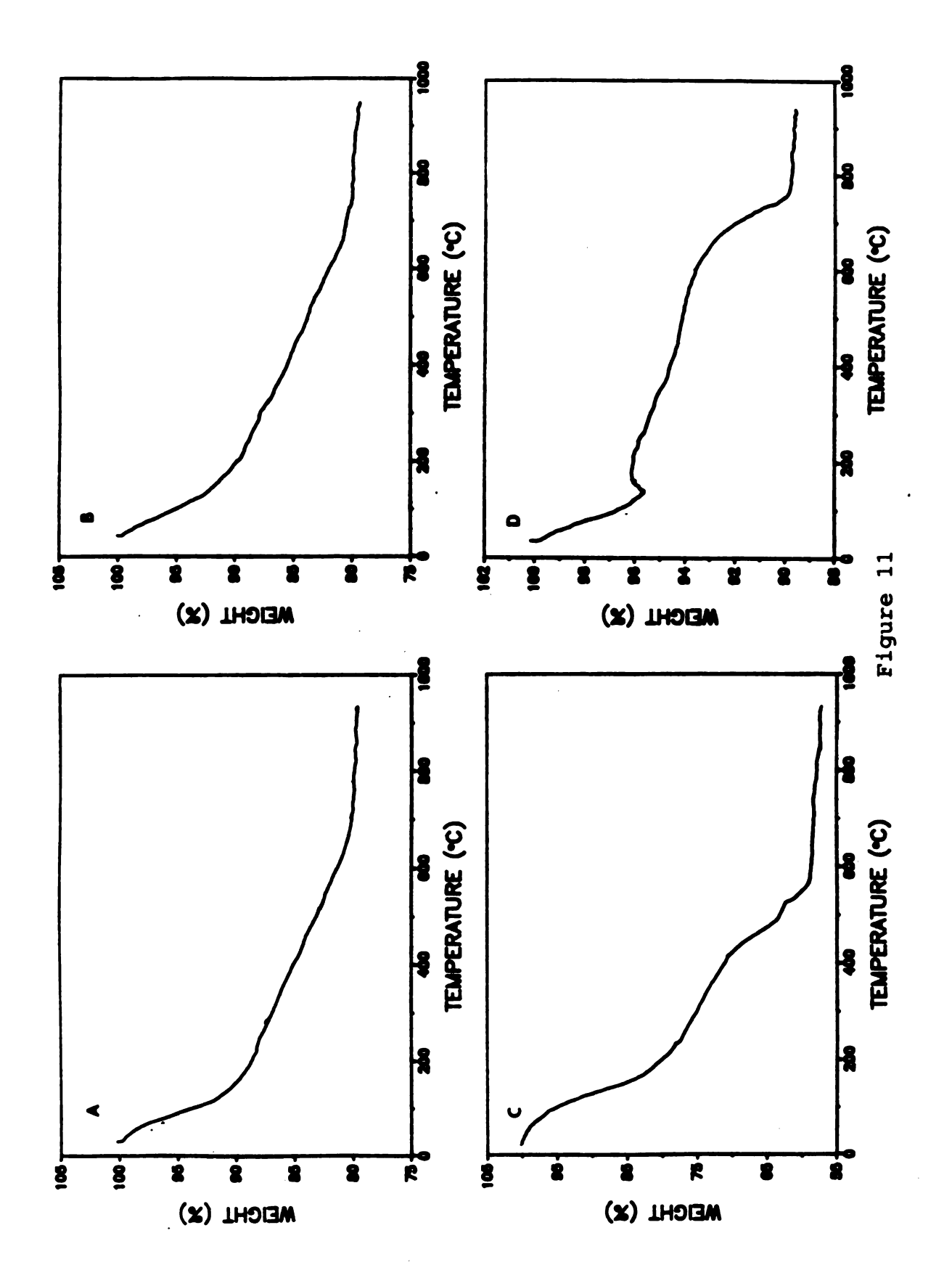


The TGA curves are given in Figure 11. Dialyzed IIM and centrifuged IIM show substantial weight loss (10%) at lower temperatures due to the removal of water, showing a slower weight loss due to tightly bound water and dehydroxylation to a temperature of 950°C. The total weight loss for the complex is approximately 20%. Imagolite losses about 20% of its total weight before reaching a temperature of 100°C due to the removal of surface water. There is also a rapid weight loss of an additional 10% at 400°C caused by dehydroxylation and partial decomposition. Imagolite losses approximately 45% of its total mass. Na+-montmorillonite shows a weight loss of about 5% from the removal of water at temperatures to 125°C. There is also a rapid weight loss starting at 600°C caused by dehydroxylation. The total mass lost by Na+-montmorillonite amounts to about 10% of its original weight.

3.3.5 Adsorption Isotherms

The adsorption properties and pore volumes for dialyzed IIM and centrifuged IIM were determined by adsorption of molecules with various kinetic diameters. The five adsorbates used were water, nitrogen, n-butane, benzene, and perfluorotributylamine. The kinetic diameters are 2.65A, 3.64A, 4.3A, 5.85A, and 10.2A respectively. Figures 12-16 show the adsorption isotherms for each adsorbate. The adsorption isotherm for nitrogen showed that the IIM samples were type 1 isotherms indicating only microporosity with no mesorphosity. Adsorption of nitrogen was very high at low p/p_0 and then leveled off at a p/p_0 equalling 0.35. The other

TGA of Dialyzed IIM(A), Centrifuged IIM(B). Dialyzed Imogolite(C), and Na⁺-Montmorillonite(D). All Samples Were Air Dried.



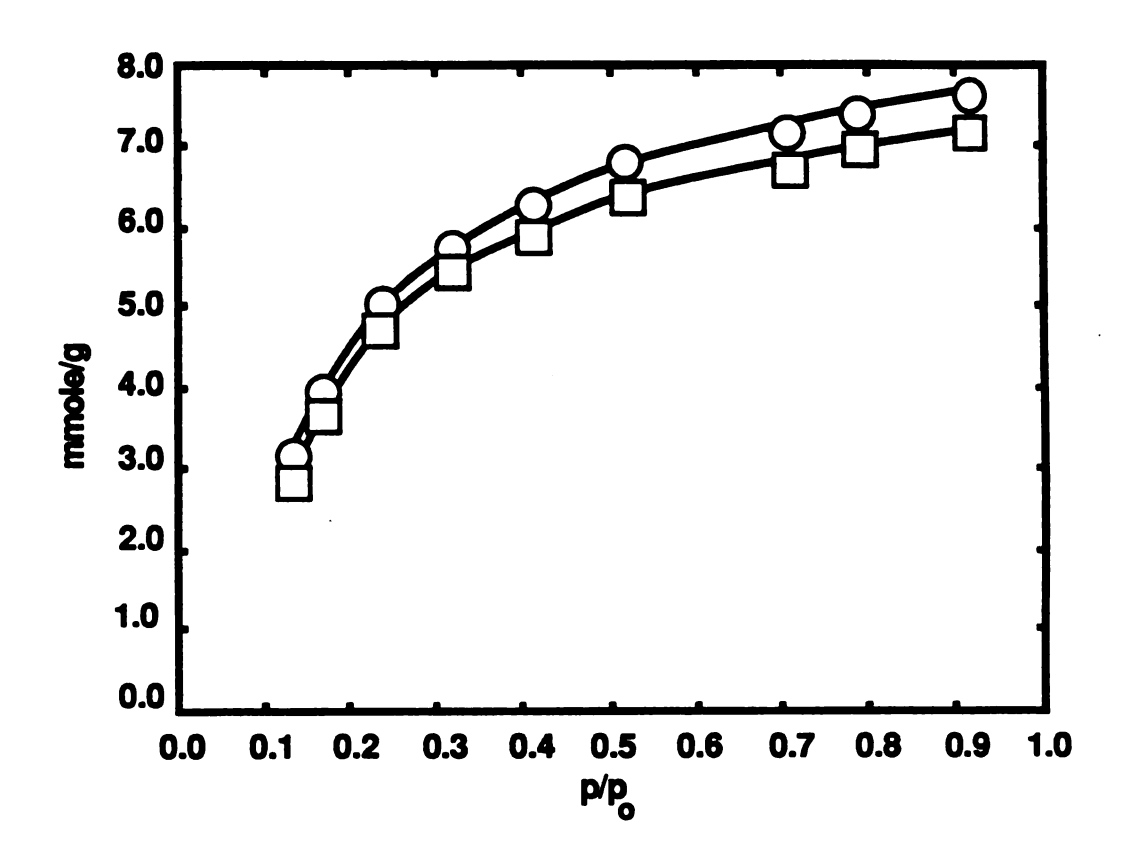


Figure 12 $\label{lem:adsorption} Adsorption \ \mbox{Isotherm of Water on Dialyzed IIM(O) and Centrifuged IIM(\Box).}$

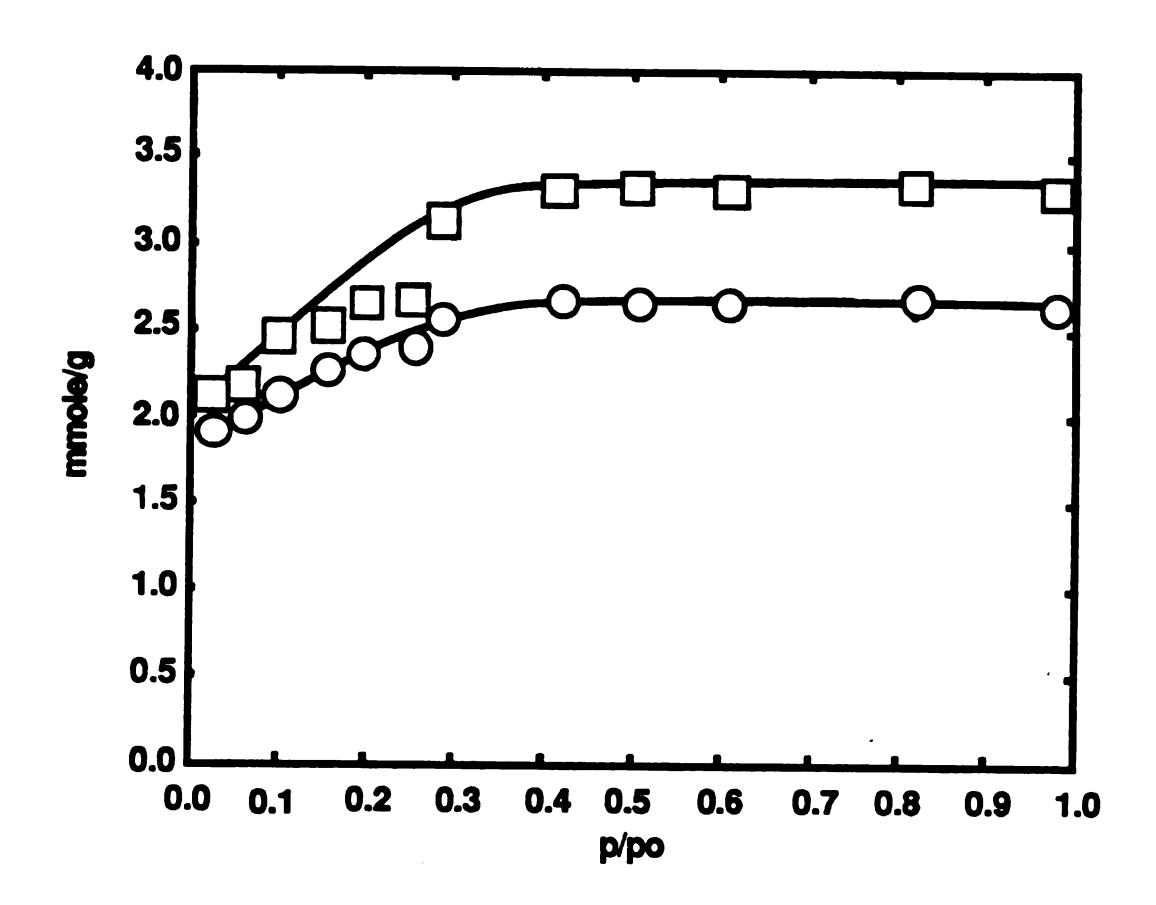


Figure 13 $\label{eq:Adsorption} Adsorption \ Isotherm \ of \ Nitrogen \ on \ Dialyzed \ IIM(O) \ and \ Centrifuged \ IIM(\square) \ .$

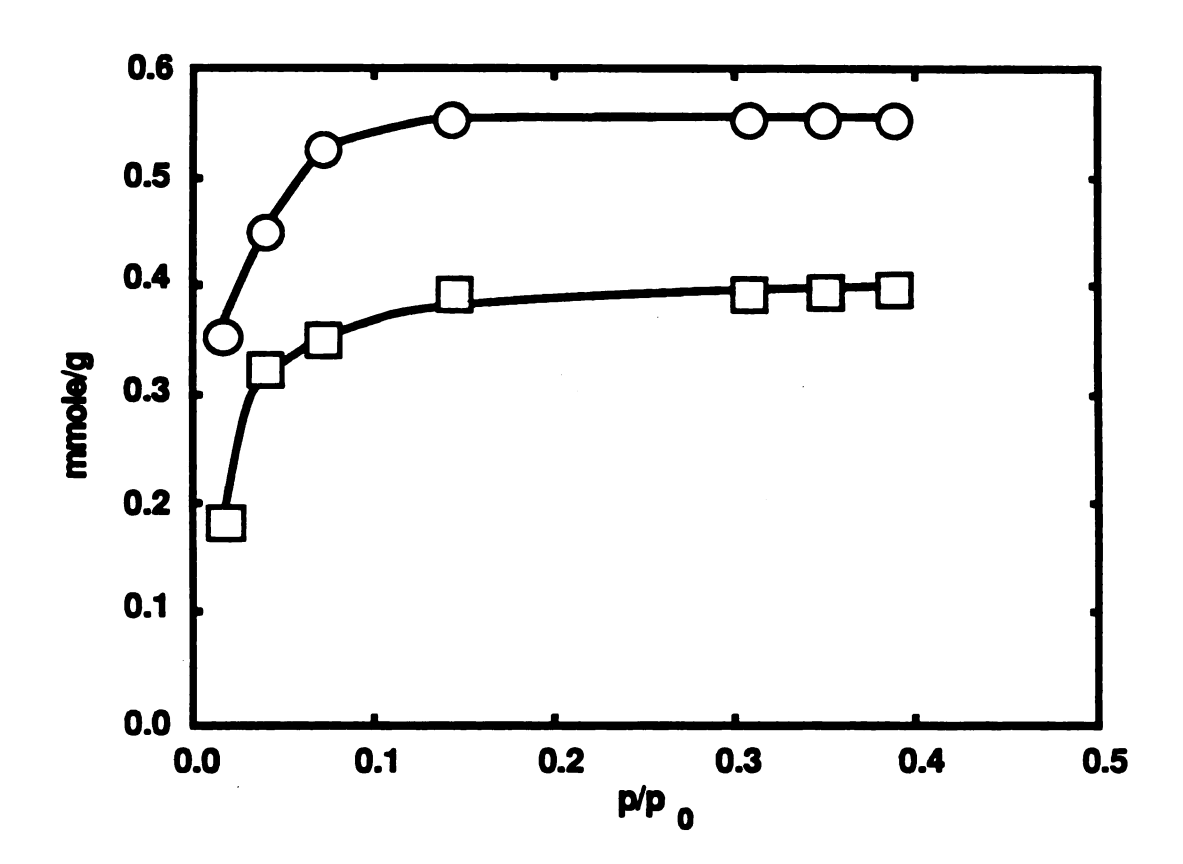


Figure 14 $\label{eq:Adsorption} Adsorption \ \mbox{Isotherm of n-Butane on Dialyzed IIM(O) and Centrifuged IIM(\square).}$

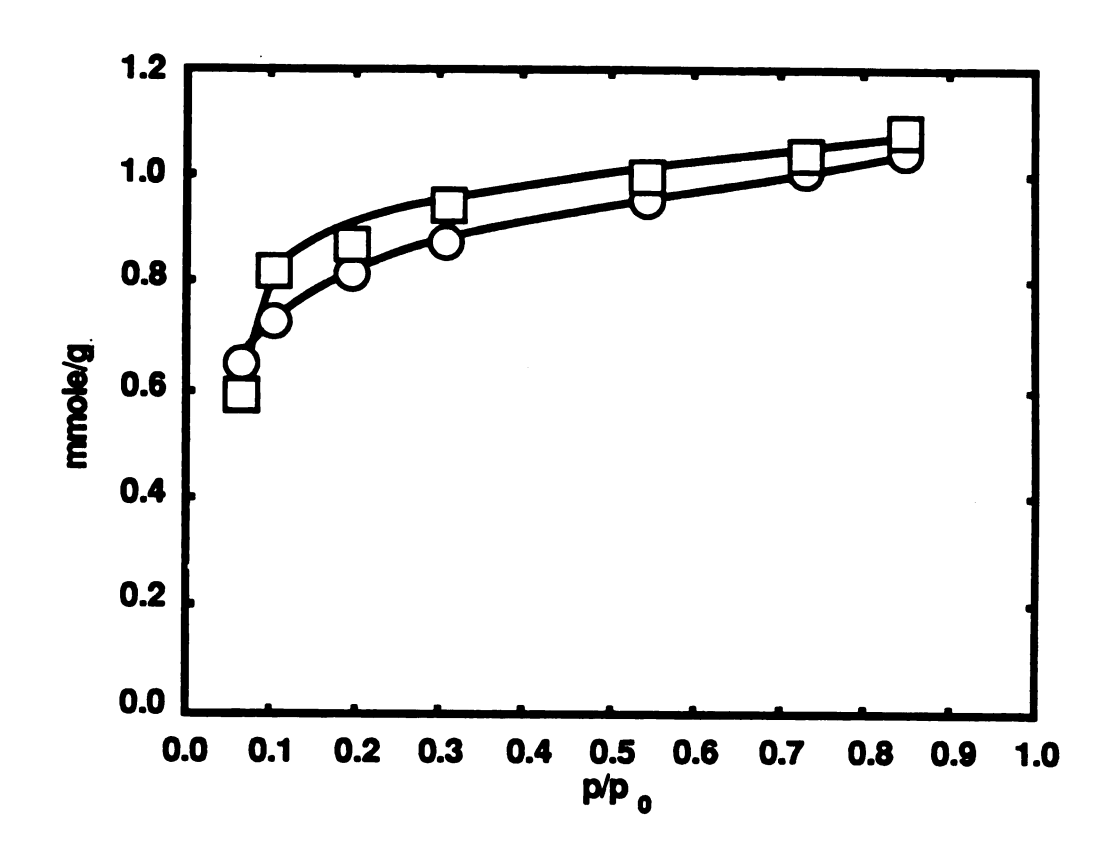


Figure 15 $\begin{tabular}{ll} Adsorption I Sotherm of Benzene on Dialyzed IIM(O) and Centrifuged IIM(\Box). \end{tabular}$

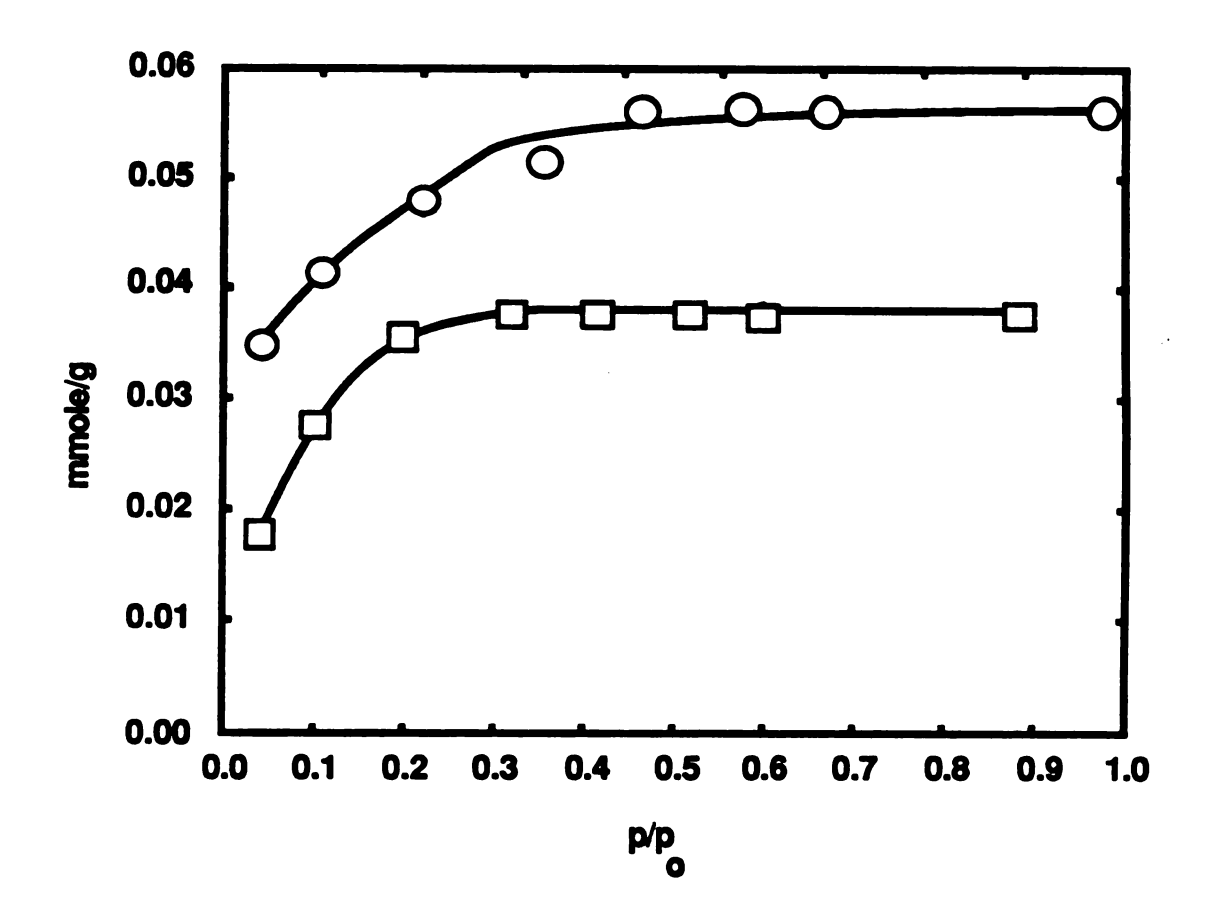


Figure 16 $\label{eq:figure 16} Adsorption \ Isotherm \ of \ Perfluorotribuytlamine \ on \ Dialyzed \ IIM(O) \ and \ Centrifuged \ IIM(\square) \ .$

adsorption isotherms were very similar, with the exception of Water showed a much slower rise in adsorption and The dependence of pore never reached a saturated maximum. volumes based on kinetic diameter are given in Table 4. The maximum pore volume is $0.137 \text{ cm}^3/\text{g}$ for dialyzed IIM and .129 cm³/q for centrifuged IIM. There is very little adsorption of perflourotributylamine due to its large kinetic diameter. the imagolite tube is only 9A while opening of perflourotributylamine has a kinetic diameter of 10.2A. The adsorption can only take place on the surface or possibly between the pillars themselves. However the exact separation of the pillars has not yet been determined. Benzene adsorbed approximately the same amount as nitrogen even though it has a much larger kinetic diameter. The reason for similar pore volumes may indicate that benzene can possibly orient itself on the surface, thus filling more pore volume than expected.

3.4 Conclusions

Elemental analysis, infrared spectroscopy, and X-ray diffraction provided evidence that imogolite could be synthesized successfully in the laboratory by the procedure described earlier in this chapter. The successful synthesis of this new material affords new possibilities in intercalation chemistry as well as catalysis. It was also shown that imogolite tubes could indeed be intercalated in the layers of Na⁺-montmorillonite. The intercalation of imogolite offers a new biphase aluminosilicate with very interesting structural properties due to the size of the basal spacing,

Table 4: Pore volumes for dialyzed IIM and centrifuged IIM based on kinetic diameters of various molecules.

<u>Sample</u>	Pore Volume	<u>Adsorbate</u>	Kinetic Diameter
Dialyzed IIM	0.137	н ₂ о	2.65
Dialyzed IIM	0.0919	N ₂	3.64
Dialyzed IIM	0.0551	C ₄ H ₁₀	4.3
Dialyzed IIM	0.0959	C6 ^H 6	5.85
Dialyzed IIM	0.0145	N(C ₄ F ₉) ₃	10.2
Centrifuged IIM	0.129	н ₂ о	2.65
Centrifuged IIM	0.115	N ₂	3.64
Centrifuged IIM	0.0393	C ₄ H ₁₀	4.3
Centrifuged IIM	0.0922	C ₆ H ₆	5.85
Centrifuged IIM	0.0217	$N(C_4F_9)_3$	10.2

these properties need further investigation in the area of catalysis. The imogolite tubes were stabilized upon intercalation as evidenced by the DTA data. The adsorption isotherms clearly indicated that IIM, however washed, is a microporous material. This microporosity offers potential for IIM to act as a molecular sieve.

CHAPTER IV

FUTURE STUDIES

4.1 Adsorption Properties of IIM

To determine the potential use of IIM as a molecular sieve, a complete survey of the adsorption properties of IIM must be studied. To obtain this information a series of adsorption isotherms must be taken using several different organic and inorganic molecules with various kinetic diameters. The pore size distribution of IIM would also be obtained, and a more complete understanding of the surface properties.

4.2 Acidity

The catalytic conversion of reactants to products for several organic reactions is dependent of the acidity of the catalyst. Because both Bronsted and Lewis acidity play such an important role in catalysis it is necessary to quantitatively measure the acidity of IIM.

The measurement of acidity depends on three factors, the number of acid sites, the strength of the acid sites, and the type of acid sites either Bronsted or Lewis. The number of acid sites can be measured quantitatively by the adsorption of a specific base (eg. ammonia, pyridine). Based on the mass of the chemically adsorbed base the number of acid sites can be determined. The strengths of the acid

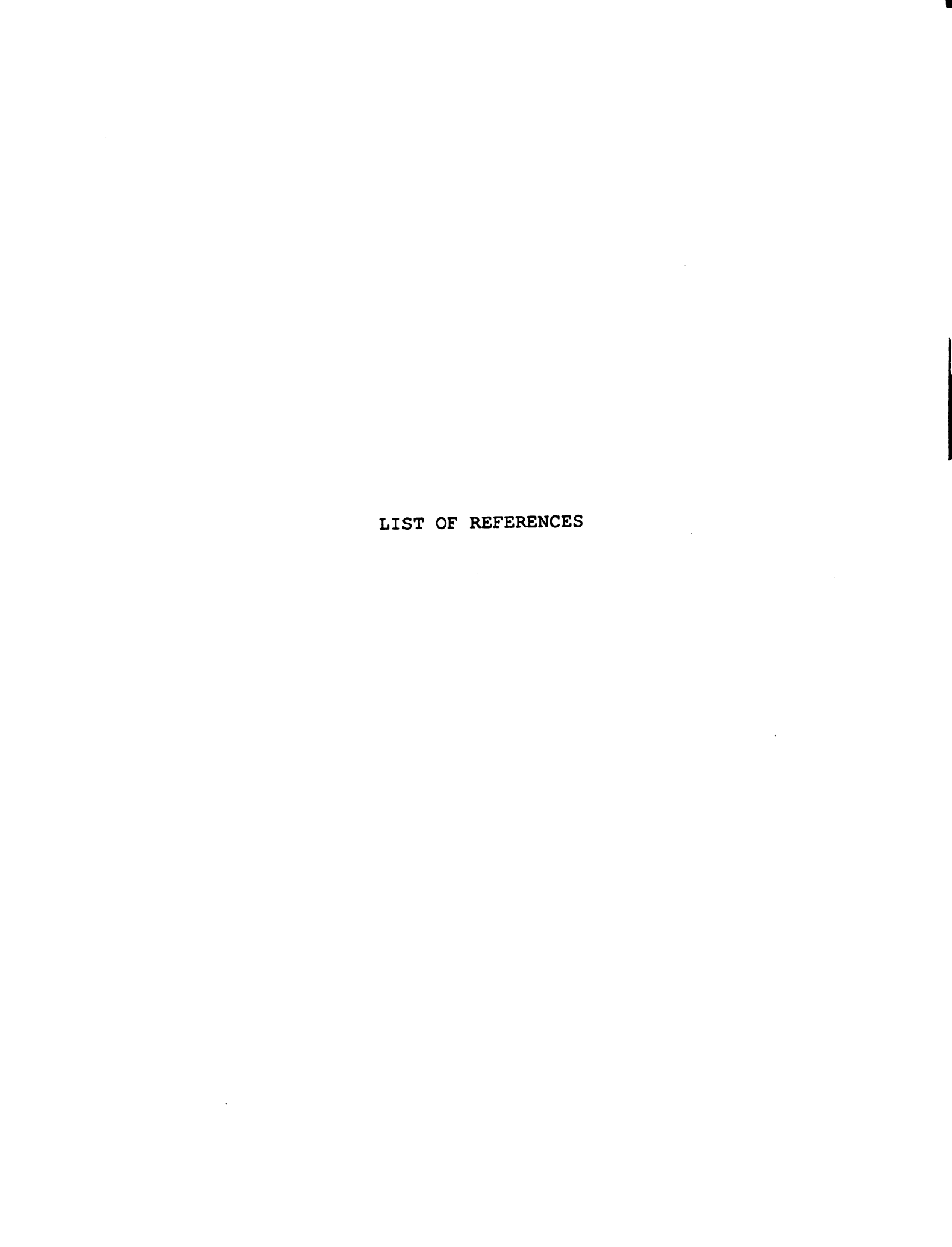
sites are determined by the amount of adsorbed base remaining at various temperatures. The base that desorbs at low temperatures is attributed to weak acid sites, while the base that desorbs at higher temperatures would indicate stronger acid sites. Although this method of measuring acid strength does not generate a quantitative number it is still useful in determining the relative percentages of strong acid sites and weak acid sites. Bronsted and Lewis acid sites can be determined by infrared spectroscopy since each unique mode of adsorption by the base corresponds to a specific infrared adsorption band. The corresponding adsorption band can then be assigned to either Bronsted or Lewis acidity.

4.3 Catalysis

Since IIM has such a large d spacing (35Å) it should offer unique opportunities for the catalysis of large molecules. The first catalytic reaction that will be studied is the dehydration of ethanol. This serves as a model catalytic reaction since the mechanisms of the two products obtained, diethyl ether and ethylene, are well known and understood. This reaction also affords the opportunity to qualitativly determine the acid strength of IIM. The second area of study would be the catalytic cracking of crude oil. The conversion and selectivity will be of interest as well as the thermal stability.

4.4 New Imogolite-Smectite Complexes

The final area of study would be the intercalation of imogolite into other smectite clay minerals. This group of minerals would include saponite, beidelite, hectorite, and possibly vermiculite. Each of these clays have different properties than montmorillonite and should offer a whole series of new catalysts or molecular sieves.



LIST OF REFERENCES

- 1. Pinnavaia, T.J. Science 1983, 220, 365.
- Barrer, R.M. "Zeolites and Clays as Sorbents and Molecular Sieves"; Academic Press, New York, 1978, 459-462.
- Mortland, M.M. and Berkheiser, V.E. <u>Clays and Clay Miner</u>.
 1978, 26, 319.
- 4. Traynor, M.F.; Mortland, M.M. and Pinnavaia, T.J. Clays and Clay Miner. 1978, 26, 319.
- Pinnavaia, T.J. In "Heterogeneous Catalysis", Shapiro,
 B.L. Editor; Texas A&M University Press: College Station,
 Texas, 1984.
- 6. Leoport Jr, R.H.; Mortland, M.M. and Pinnavaia, T.J.

 Clays and Clay Miner. 1978, 27, 201.
- 7 Brindley, G.W. and Semples, R.E. <u>Clay Minerology</u> **1979**, 12, 229.
- 8. Yamanaska, S. and Brindley, G.W. Clays and Clay Miner.

 1978, 26, 21.
- 9. Johnson, G. Acta Chem Scand. 1960, 14, 661.
- 10. Landau, S. Ph.D Dissertation, Michigan State University.1984
- 11 Theng, B.K.G. "The Chemistry of Clay-Organic Reactions;" Wiley, New York, 1974.

- 12. Van Olphen, H. "An Introduction to Clay Colloid Chemistry;" Wiley, New York, 1977.
- 13. Tilak,D; Tennakoon, B.; Jones, W. and Thomas, J.M.

 J.Chem. Soc. Farraday Trans.1.,1986, 82, 3081.
- 14. Whithurst, D.D. J.Chem. Tech. 1980, 44.
- 15. Endo, T.; Mortland, M.M. and Pinnavaia, T.J. Clays and Clay Miner. 1980, 28, 105.
- 16. Dixon, J.B. and Weed, S.B. "Minerals in Soil Environments;" Soil Science Society of America, Madison, Wisconsin, 1977.
- 17. Russel, J.D.; McHardy, W.J. and Fraser, A.R. <u>Clay</u>
 Minerals, **1969**, 8, 87-88.
- 18. Cradwick, P.D.G.; Farmer, V.C. and Russell, J.D. Natural

 Physical Science, 1972, 240, 188.
- 19. Goodman, B.A. et al. <u>Phys. Chem. Minerals</u>, **1985**, *12*, 342-346.
- 20. Farmer, V.C. U.S. Patent 4252779, 1981.
- 21. van der Gaast, S.J.; Wada, K.; Wada, S.I. and Kakuto, Y.

 Clavs and Clav Minerals, 1985, 33, 237-243.
- 22. Wada, K. "Minerals in Soil Environments", Soil Science Society of America, Madison, Wisconsin, 1977.
- 23. Henmi, T. and Wada, K. Clay Miner. 1974, 10, 231-236.
- 24. Pinnavaia, T.J. and Johnson, I.D. U.S. Patent 4621070A, 1986.
- 25. Farmer, V.C. and Fraser, A.R. <u>Developments in Sedimentology</u>, **1978**, *27*, 547.

MICHIGAN STATE UNIV. LIBRARIES
31293005798073